UiT The Arctic University of Norway

Faculty of Biosciences, Fisheries, and Economics

Department of Arctic Marine Biology

Seasonal changes of intertidal benthic microalgae photoacclimation during the summer to mid-winter transition period on Tromsøya

Emily Reast

BIO-3950

Master's thesis in Biology, May 2024

Seasonal changes of intertidal benthic microalgae photoacclimation during the summer to mid-winter transition period on Tromsøya

Author: Emily Reast

Supervisors: Rolf Gradinger (UiT)
Markus Molis (UiT)

Open paper

May, 2024

Acknowledgements

I would like to express my deepest gratitude to my supervisors, Rolf Gradinger and Markus Molis, for their invaluable guidance, patience, and teaching. It has truly been a wonderful experience to have the opportunity to have you as mentors here at UiT and during my introduction to the field of marine biology/intertidal zone work.

I would also like to thank fellow master's students (Judith, Robin, Freddy, Malou, Femke) who shared their time to help me fix problematic R codes, explain biological concepts I was struggling to understand, and for providing me with much needed moral support. Thank you also to all the friends I've made while at UiT for making me feel at home here in Tromsø and to my family and friends back in Alaska who's never ending love and support has been immeasurable.

This degree would also not have been possible without the support I received during my bachelor's degree from my mentors at the University of Alaska Fairbanks. Words cannot express my gratitude to Syndonia Bret-Harte, Jackson Drew, and Diane Huebner who supported my first steps into the world of academic research biology and arctic biology fieldwork.

Table of Contents

List of Tables

List of Figures

Abbreviations, acronyms, and relevant symbols

MPB	Microphytobenthos
Chl *a*	Chlorophyll *a*
PAM	Pulse Amplitude Modulated (technique for measuring algal activity)
PAR	Photosynthetically active radiation
RLC	Rapid light curve
PSII	Photosystem II
α	Alpha: the initial slope of a rapid light curve (µmol photons $m^{-2}s^{-1}$)
ps ($rETR_{max}$)	Maximum relative electron transport rate (µmol electrons $m^{-2}s^{-1}$)
E_k	The photoacclimation parameter (sometimes called I_k) (µmol photons $m^{-2}s^{-1}$)
F_0	Minimum chlorophyll fluorescence when algae is in dark-adapted state(RFU)
Q_{max}	Maximum quantum yield when algae is in dark-adapted state

Abstract

The microphytobenthos (MPB), defined as the microscopic photosynthesizers inhabiting sediments in marine and estuarine environments, are a vital component to intertidal ecosystems. They contribute greatly to ecosystem services in many ways and are responsible for a high amount of primary productivity in their environments. Microphytobenthic abundance and community structure studies have been increasing in the Arctic, but there is still a lack of knowledge and understanding of how they function at high latitudes. Polar regions exhibit high variability in light and temperature conditions throughout the year, but microalgae have impressively adapted to be able to thrive in this variable climate.

Seasonal studies on changes in MPB abundance have been performed in polar regions, but most focus on spring and summer months and the transitions between them. This study aims to better understand temporal responses of the MPB from late August to mid-December in the intertidal zone on the island of Tromsøya, located in Northern Norway. Through this project, the topics of overall MPB abundance and community structure are examines to address whether there is visible seasonality within these communities. Surface sediment samples from September and December 2024 were examined through microscopy to obtain overall live cell counts as well as identify the various taxa that make up the intertidal microalgae here. Chlorophyll fluorescence measurements were carried out weekly using a hand-held fluorometer, allowing for the calculation of rapid response light curves and their relevant parameter estimates which inform us about algal physiology. Additionally, weekly sediment samples were analysed for chlorophyll *a* (Chl *a*) content.

Results suggest that there is indeed some seasonality aspect within the intertidal MPB on Tromsøya from late August to mid-December. There appears to be a shift to slower photosynthesis and also a lower light requirement from the algae later in the sampling season. Furthermore, taxa compositions are comparable to those of other coastal areas in the Arctic. Further studies are still needed to obtain a more complete understanding of the MPB in Northern Norway and on Tromsøya as there were many unexplored environmental factors in this study.

Key words: Arctic – microphytobenthos – microalgae – Chlorophyll *a* – primary productivity – intertidal – field study

1 Introduction

1.1 Microphytobenthos: an important component in marine food webs

Microphytobenthos (MPB) are commonly defined as communities of photoautotrophic cyanobacteria and microalgae that inhabit illuminated benthic aquatic habitats (Serôdio & Paterson, 2022). The MPB may provide as much as one third of total primary production in estuarine systems, and they also contribute to sediment stabilization, nutrient and trophic fluxes in intertidal soft sediments, enhancement of water quality through nutrient recycling and removal, and retention of pollutants (Pinckney & Zingmark, 1991). They provide a food source to birds and other animals and support an environment which supports human recreation (Pinckney & Zingmark, 1991). Thus, MPB provides a wide range of ecosystem services. Furthermore, due to their high productivity and location at the land-sea interface, intertidal MPB play an important role in determining how and how much carbon is available to surrounding ecosystems, including ocean ecosystems (Oakes et al., 2016). The MPB support both benthic and pelagic food webs, in part due to the ability of these microalga to alter their biomass so quickly (Blanchard et al., 2001). It can be hypothesized that the seasonal productivity changes of MPB will increase with latitude due to the high amount of sunlight in summer, but a clear understanding of the ranges in rates of benthic productivity with latitude has not yet been observed (MacIntyre et al., 1996, Attard et al., 2024). Therefore, the base of this project centering on the MPB around Tromsø will primarily focus on the seasonality of MPB abundance and growth potential through looking at their photoacclimation in a seasonal context.

In their natural environment, benthic microalgal communities typically form biofilms, which are characterized by thin layers with high abundances and intense vertical and horizontal gradients in physical, chemical, and biological properties (Salleh & McMinn, 2011). In intertidal zones, motile diatoms typically form a large part of these biofilms in the top 1-2 millimeters of sediment during low tide periods (MacIntyre et al., 1996). Moreover, high abundances of benthic microalgae, flagellates, ciliates, and meiofauna organisms are commonly found in this relatively thin and oxic layer of top sediment (Böttcher et al., 2000). Interestingly, MPB performs daily migrations, typically thought to align with tidal and daylight cycles (Launeau et al., 2018). At the beginning of each daytime low tide exposure period, surface sediment chlorophyll *a* (Chl *a*) concentrations increase rapidly as this biofilm forms, and the biofilm disappears completely at the end of the daytime exposure period, when the microalgae burrow into the sediment or the biofilm is resuspended into the water column (Guarini et al., 2006). Additionally, while light has the power to attract MPB to the sediment surfaces, it can also cause them to sink lower into the sediment to avoid photodamage if irradiance is too high (Perkins et al., 2002).

1.2 Arctic microphytobenthos studies and knowledge

The number of studies being done on Arctic microphytobenthos (MPB) has been increasing, although there remain many gaps due most studies focusing on other areas of the world with less variation in light and temperature conditions (Cahoon, 1999). With decreasing ice-covered benthic environments in the Arctic, the availability of suitable conditions for MPB

growth has been increasing, but there is still a lack of understanding on this topic in the Arctic (Attard et al., 2024). Due to the size and sometimes inaccessibility of studying in the Arctic, a comprehensive analysis of benthic primary productivity is mainly inferred through models (Attard et al., 2024). However, the Arctic alone has more than 250,000km of coastline, offering a large area for the MPB to inhabit (Jakobsson et al., 2020). This constitutes 24.1% of the global coastline, and 14% being an environment ideal for MPB (Gattuso et al., 2020). The Arctic in fact provides a very suitable habitat for benthic microalgae and can maintain high biomass and primary productivity in the intertidal and subtidal zones despite having a characteristically short growing season and cold temperatures (Pessarrodona et al., 2022). Arctic benthic microalgae actually have a similar amount of primary productivity to shallow pelagic (<30m) coastal ecosystems (Glud et al., 2009). While it is true that low temperatures and light levels can suppress primary productivity, Arctic MPB typically are highly adaptable (Oakes et al., 2016). In general, polar algae have a striking ability to photosynthesize and grow under extreme conditions including very low irradiance and temperatures (Gómez et al., 2009). Therefore, unique acclimations and adaptations of Arctic MPB can be expected and transferring the behavior of benthic microalgae at lower latitudes to Arctic microalgae can lead to wrong conclusions.

Diatoms are typically the most common primary producers on Arctic sediments (Woelfel et al., 2010). High latitude diatom species are adapted to Arctic to light and temperature conditions, and also have the advantages of rapid colonization, motility, and various light exposure control techniques (Cohn et al., 2016, Jesus et al., 2023, Attard et al., 2024). The impressive evolutionary adaptations, both structurally and behaviorally, these diatoms have gained allows them to thrive in environments such as the Arctic (Goessling et al., 2018, Cartaxana et al., 2016).

Particularly regarding the movement within the microphytobenthos' sediment surface in polar regions, knowledge on this topic is still lacking and developing (Karsten et al., 2019). In an area of the world which experiences such drastic fluctuation in light availability, it is thought that the MPB experiences light-limitation, rather than nutrient limitation, and that light availability could be a decent proxy for estimating benthic primary productivity (Glud et al., 2009). Furthermore, recent models determine that 50-60% of the annual benthic primary productivity of microalgae occurs in July and August, when seawater is more transparent due to a decrease in terrestrial runoff and limitation of phytoplankton growth from decreased nutrient availability, but the analysis of the transition period into winter is less commonly studied (Attard et al., 2024). Furthermore, minimum light requirements for the MPB have not been clearly determined even though benthic diatoms have been found down to depths of almost 200 meters where the maximum light availability was 0.2µmol photons $m^{-2}s^{-1}$ (McGee et al. 2008). Therefore, a main objective for carrying out this project was to add to the existing arctic knowledge on coastal microphytobenthic systems and behavior, particularly focusing on this transition period into winter conditions.

1.3 Estimating MPB abundance and community composition

There are various accepted ways to measure abundance of the microphytobenthos (MPB), some of which have been used more than others in previous studies. Many past studies have used benthic Chl *a* alone as a measure for total community biomass, but the inclusion of community structure is becoming increasingly common in studies trying to understand the functioning of MPB biofilms (Malakhov, 2021). This study includes both Chl *a* analysis and

microscopical determined microalgal abundances to gain community structure information since it will lead to both more accurate and holistic results (Cibic et al., 2007).

There are many ways to measure algal activity and photophysiology, but a common method used for the intertidal MPB involves the use of a hand-held fluorometer to measure activity at photosystem II (PSII) within algal chloroplasts. The use of the Pulse Amplitude Modulated technique (PAM) to obtain indirect measures of Chl *a* from the chlorophyll fluorescence kinetics and photosynthetic activity within microalgae has also been increasingly included in many studies due to its rapid, non-destructive, and portable use (Forster et al., 2003, Consalvey et al., 2005). Photosynthetic quantum yield, defined as the amount of photosynthesis at a certain irradiance per quanta of light (photons) absorbed by the photosynthetic pigment (Chl *a*), is the basic measurement taken with this method (Saroussi & Beer, 2007). Essentially, the PAM method involves exposing the algae to modulated light pulses (the irradiance) that allow for chlorophyll fluorescence measurements (quantum yield) without having induced photosynthesis (McMinn & Hegseth, 2004). The results allow for calculation of the relative electron transfer rate (rETR) within PSII, the creation of rapid light curves, and thus their fluorescence parameters which can be extremely helpful in determining biomass and understanding the photoadaptive state of algae (Consalvey et al., 2005, McMinn & Hegseth, 2004).

1.4 Goals and hypotheses of this project

This master's project aims to explore and better understand the seasonal activity and community structure of the microphytobenthos in a high latitude intertidal zone close to Tromsø by tracking and measuring photosynthetic parameters, species presence, and abundance through variable fluorescence approaches, sediment sample cell counts and Chl *a*. This study also aims to assess the degree to which seasonality within these parameters may occur. The main objectives of this study can therefore be split into two

1. to investigate how the microphytobenthos abundance and composition changes from late August (polar day conditions) to mid-December (polar night conditions) through microscopy work with sediment samples.

   Hypotheses:

   - Diatoms will remain the dominant taxa in samples from both August and December, constituting at least 90% of identifiable taxa.
   - Overall abundance, measured with live cell count data, will decrease from August to December.

2. to look at photosynthetic activity, based on fluorescence quantum yield, rapid response light curve measurements, and Chl *a* measurements from sediment samples, of the microphytobenthos change over time, within the period from late August to mid-December.

   Hypotheses:

- Average dark-acclimated maximum quantum yield measurements will demonstrate high values at the beginning of the sample season but decrease with daylight throughout the sample season.
- Rapid response light curve parameters will indicate a slower rate of photosynthesis (as seen through a change in initial rate in relative electron transport rate in photosystem II) and a higher light requirement (as seen through the required light intensity to reach the maximum relative electron transport rate using the above rate).
- Chl *a* values from sediment samples will decrease in concentration from August to December.

2 Materials and Methods

2.1 Study Site

All field sampling was conducted within a 200m range located in an intertidal zone located on the island Tromsøya in Northern Norway (69.67˚N 18.90˚E, Figure 1) between August and December 2023. At the sample site, the intertidal zone extends horizontally several hundred meters from the low to the high-water mark. As characteristic of high latitude locations, this site experiences extreme seasonal variation in hours of daily sunlight, air temperature, and seawater temperature. The tidal range during my study period varied from 25cm (maximum low water) to 288cm (maximum high water), with two tidal cycles per day (www.kartverket.no, 2023).

The sampling site was located in an area of the intertidal zone which displayed a patchy distribution of macroalgae, primarily *Fucus vesiculosus,* and exposed fine-grained sediment. This area was selected due to the easy accessibility from land and the presence of abundant soft sediment habitat for microalgal biofilms.

Although seemingly unaffected, it should be noted that some of the sample plots were roughly 150m away from an active construction project on the beach for about two months of the field sampling period. There was no visual evidence of physical alterations, such newly introduced surface sediments or footsteps, to the sampling location from this activity.

2.2 Experimental design

The field measurements were conducted in two blocks, representing two areas roughly $10m^2$ in area within the mid-shore intertidal zone along the same beach and with variation in freshwater exposure due to proximity of a freshwater creek (confirmed with salinity measurements). Each block contained three plots (0.5 x 0.5m) from which sampling directly occurred. GPS locations (Table 1) for each plot were taken with an iPhone 12 mini in the field before sampling began. The block sites were chosen due to the visually homogenous quality of the sediment grain size and surface texture, only containing minimal amount of macroalgae (since microalgae was the focus of this study), and being within the tidal zone dominated by *Fucus vesiculosus*. The three plots were assigned randomly and were marked in each block with two tagged metal rods marking two corners of the square plots. The distance between the plots was ca 5m.

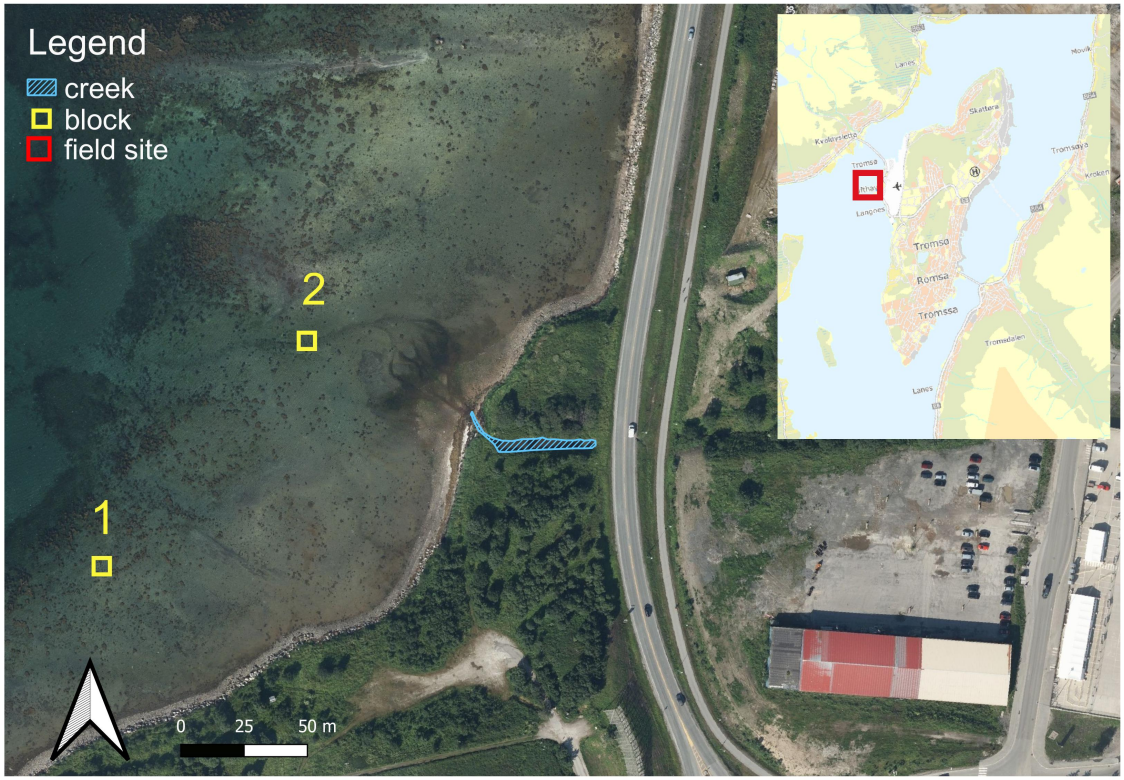

***Figure 1**. Aerial photo of sample site on the west coast of Tromsøya in northern Norway. The two blocks from fieldwork are marked with yellow in the photo above, and the freshwater stream marked with light blue. Block 1 and block 2 were ca 100m distance from each other with block 2 in proximity to the inflow of a small freshwater creek. The influence of this flow was also distinguished by a large nearby patch of* Ulva intestinalis*, a green alga common in brackish water areas.*

***Table 1:** Plot Locations were recorded with coordinates in decimal degrees and physically marked with metal rods in two corners for easy resampling and identification. B=Block number (1 or 2) and P=plot number (1, 2, or 3).*

Plot ID	Coordinates (decimal degrees)
B1P1	69.67981°N 18.89783°E
B1P2	69.67983°N 18.89792°E
B1P3	69.67979°N 18.89782°E
B2P1	69.68063°N 18.89853°E
B2P2	69.68061°N 18.89861°E
B2P3	69.68061°N 18.89844°E

2.3 Sampling

2.3.1 Sampling Overview

Weekly sampling was carried out from August 31st through December 14th, centered around low tide cycles closest to solar noon. Samples taken for later microscopy examination were taken on September 20th and December 14th, 2023. In total, this project included 16 complete weekly sampling events to address the seasonality of microphytobenthos properties (research question 2, Table 2). The selected days for fieldwork were chosen based on the need for sufficient time to conduct all measurements within one tidal cycle, and predicted weather conditions (www.yr.no, n.d.) for that day.

Table 2: *Complete list of all sample days with time in field, daylight amount, and tide information (tide information from www.kartvertet.no, daylight information from NOAA's Solar Calculator).*

Date:	Time period of sampling (first and last Aquapen measurement)	Sample day count	Low tide (time)	Day length (hours and minutes)
August 31, 2023	8:44-10:50	Sample day #1	8:24	15 hrs 35 min
September 7, 2023	12:34-15:18	Sample day #2	13:39	14 hrs 34 min
September 15, 2023	7:19-10:06	Sample day #3	8:42	13 hrs 25 min
September 20, 2023	9:42-12:30	Sample day #4	11:16	12 hrs 43 min
September 29, 2023	7:12-9:35	Sample day #5	8:02	11 hrs 27 min
October 3, 2023	9:54-12:17	Sample day #6	10:45	10 hrs 53 min
October 13, 2023	6:21-8:53	Sample day #7	7:39	9 hrs 28 min
October 16, 2023	8:08-10:34	Sample day #8	9:07	9 hrs 2 min
October 27, 2023	6:11-8:42	Sample day #9	6:53	7 hrs 23 min
November 1, 2023	7:54-10:27	Sample day #10	9:17	6 hrs 35 min
November 6, 2023	12:45-14:11	Sample day #11 (incomplete)	13:54	5 hours 45 min
November 10, 2023	16:31-18:53	Sample day #12	17:40	5 hours 4 min
November 15, 2023	7:11-9:30	Sample day #13	8:15	4 hrs 7 min
November 21, 2023	12:24-14:49	Sample day #14	13:41	2 hrs 49 min
November 30, 2023	7:44-10:26	Sample day #15	8:57	0 hrs 0 min
December 7, 2023	14:03-16:20	Sample day #16	15:06	0 hrs 0 min
December 14, 2023	6:55-9:13	Sample day #17	8:00	0 hrs 0 min

2.3.2 Sampling for quantitative analysis of microalgal composition and abundance

Surface sediment samples were taken in the form of small 1cm deep sediment cores taken with an open-ended plastic syringe (3cm inner diameter) from within in each plot, as done in previous studies (Woelfel et al., 2010 and Pinckney & Zingmark, 1991). One core was taken from each of the six plots on September 20th and December 14th during weekly fieldwork. Each sediment sample was placed in a 50mL plastic falcon tube in which the sample remained until later examination via microscopy for composition and abundance analysis at the university. The sample locations within the plots were randomly selected ahead of fieldwork and were different in each plot. Upon collection, 2.5ml of 37% formalin was added to the collection tube and mixed thoroughly, by manually overturning of the sealed tube, to preserve the state of the algae before storage in the university refrigerator.

2.3.3 Sampling for weekly assessment of microphytobenthos photophysiology

At each sampling event, three replicate rapid response light curve measurements in each plot (9 measurements in each block) were taken. These measurements were taken using the PSI-AquaPen-P AP 110-P (simply referred to as AquaPen hereafter), a handheld active fluorometer which assesses photosynthetic performance of microalgae by determining the photosynthetic quantum yield at 7 different irradiances, thus producing a rapid response light curve. The AquaPen derives photosynthetic activity from the chlorophyll fluorescence kinetics based on the Pulse Amplitude Modulated technique (PAM) and also provides an indirect measure for Chl *a* (AquaPen Instruction Guide, 2023, p.6). It provides a non-invasive and fast assessment of photosynthetic parameters of intertidal benthic microalgae and has been considered an acceptable tool for such measurements in previous studies (Forster et al., 2003). Prior to each measurement, an opaque plant pot was placed up-side down for 5 minutes at each location to be sampled under the AquaPen probe.
This step ensures the opening of all reaction centers within photosystem II, allowing for the assessment of the maximum quantum yield of dark acclimated samples. Following the dark acclimation step, the AquaPen was inserted into a hole made on the bottom of the upside-down cup with the sensor situated just above the sediment surface. The AquaPen was left undisturbed in this position for roughly 7.5 minutes to carry out an LC3 measurement. Each LC3 measurement consisted of seven successive measurements in phases of sixty seconds whereby the sediment surface was illuminated with light pulses increasing in intensities (10, 20, 50, 100, 300, 500, 1000 $\mu mol.m^{-2}s^{-1}$) between each quantum yield measurement.

Figure 2: Photo from sampling on October 13th, 2023. The tips of the two metal rods marking this plot are visible in the top left and bottom right corner. The plastic tube plot identification square is sitting on the sediment surface to aid in correct sampling locations. There are two upside down cups pushed into the sediment: the cup on the left is holding the AquaPen during the process of an LC3 measurement, and the cup on the right is covering the next sample spot in complete darkness for the duration of the current LC3 measurement.

In addition to the rapid response light curve measurements, data collection included the determination of irradiance (PAR, photosynthetic active radiation) measurements at the beginning and ending of working in each block with a LI-1000 DataLogger connected to a 2pi surface PAR sensor. Air and sediment temperatures at the time of each LC3 measurement were taken using a VWR waterproof precision thermometer (TD20) with a ø 3mm fixed immersion probe which was consistently placed about half a centimeter deep into the sediment surface and additionally held in a shaded location for air temperature readings. Salinity and water temperatures for the water in each block, ocean water closest to that block, and also the freshwater creek which flows near block 2 were measured with a Pro30 YSI conductivity meter deployed in shallowly dug pits near blocks 1 and 2 and in the nearest seawater to each block to obtain the ocean salinity of the nearest seawater.
Sediment core samples for later determination of Chl *a* concentrations were taken from the top 1cm of sediment, using the same open-ended syringe method as with the microscopy

sample collection from each plot. Samples were stored in 50mL falcon tubes for transport and stored at –20˚C back at the university until analysis.

2.4 Lab work

2.4.1 Microscopic determination of microalgal composition and abundance

Microscopic assessment of community composition and live algal cell abundance was performed on two sampling events (September 20th and December 14th) due to time constraints. From each plot, 1cm deep sediment cores were collected during fieldwork using the open syringe method (see above) and combined with 42.5ml filtered seawater to a total volume of exactly 50mL and then mixed by manually turning over the tube repeatedly for 5 minutes. The tubes were then set in a stand for 30 seconds to allow bigger inorganic and heavy sediment particles to settle before pipetting 2.5mL water volume into an Utermoehl chamber. Some of the samples still contained too much inorganic sediment for microscopic analysis and therefore were further diluted with 5mL of seawater before taking a second 2.5ml sample.

A Zeiss Primovert microscope was used with the 400X magnification to count microalgae. Twenty fields of view were analyzed from each sample, in which cells alive at the time of fixation were counted and all microorganisms were grouped into general taxa categories and noted. Empty diatom frustules were not included in any microscopy counts, but broken frustules in which over half of the probable original size remained were counted, as done by Scholz & Einarsson (2015).

2.4.2 Analysis of chlorophyll *a* concentrations

To assess chlorophyll content, frozen sediment samples were weighed in their collection tubes before being thoroughly mixed, via manually shaking and vortexing for 5 seconds, with 5mL of 100% acetone as an extractor. Sediment samples were then centrifuged (Eppendorf centrifuge 5702 R model) for 3 minutes to gather all the sediment particles within the liquid of the tube and ensure that the extraction was done including all the sediment in the tube. Samples were then returned to the freezer at –18˚C in complete darkness for 24 hours whilst the extraction occurred. All samples were then put in the centrifuge for 10 minutes at 4000 rotations per minute before extracting a 60 µL subsample and diluting it with 3mL of 100% acetone. These diluted subsamples were placed in glass vials, shaken by hand while covering the top with parafilm, and then placed in the Turner Trilogy lab fluorometer for raw before acidification (Rb) fluorescence measurements. After the Rb measurement, 2 drops of 10% HCl were added to each sample, followed by another physical mixing via shaking, before obtaining the raw after acidification (Ra) fluorescence value. Two blank vials, one of pure 100% acetone and the other containing 100% acetone mixed with 2 drops 10% HCl, were always measured at the beginning of every lab session for later use in calculation of final chlorophyll values.

Once all chlorophyll fluorescence values were obtained, all the sediment samples were fully dried in the fume hood and with the help of a Termaks drying oven. The tubes were then completely emptied before obtaining the clean and dry weight of each tube. From this, it was possible to calculate the frozen weight of each sample by subtracting the weight of the tube

from the initial recorded mass of the tube and frozen sample together. This was included in the methods to double check a consistent sediment sample amount because field work conditions created variation in sediment consistency while sampling.
Using the obtained raw chlorophyll fluorescence values, the blank values, and the appropriate dilution factor, the Chl *a* concentrations could then be calculated using the equation below.

$$\text{Chl a } (\mu g/L) = Fd^* \tau^* (Rb-Ra)^* VolSolvent/VolWater$$

Fd = 0.000365 (µg/L, from slope of calibration curve)
τ (tau) = 2.082

Figure 3: *τ (tau) is the average ratio of Fo/Fa for all samples and is derived from the samples used when calibrating the fluorometer. τ remains the same until the next time the fluorometer is calibrated, and the most recent calibration was in June, 2023) (Bos & Keyzers, 2023) (all volume measurements entered in L)*

2.5 Estimation of photosynthetic performance parameters based on the active fluorometer measurements

The downloaded data from the AquaPen was used to calculate the relative electron transport rates (rETR, or relative ETR, in µmol photons $m^{-2}s^{-1}$) for each light curve taken throughout the season. For each measurement, the relative electron transport rate (rETR) at each light intensity within the rapid response light curve was calculated in Excel. This was done by multiplying the light intensity of each light pulse by the determined quantum yield (from AquaPen) and then multiplying again by .5 (light fractionation between photosystem I and II). With the rETR values, photosynthetic irradiance parameters were fitted to the available rETR data, based on the equation developed by Eilers and Peeters (1988).

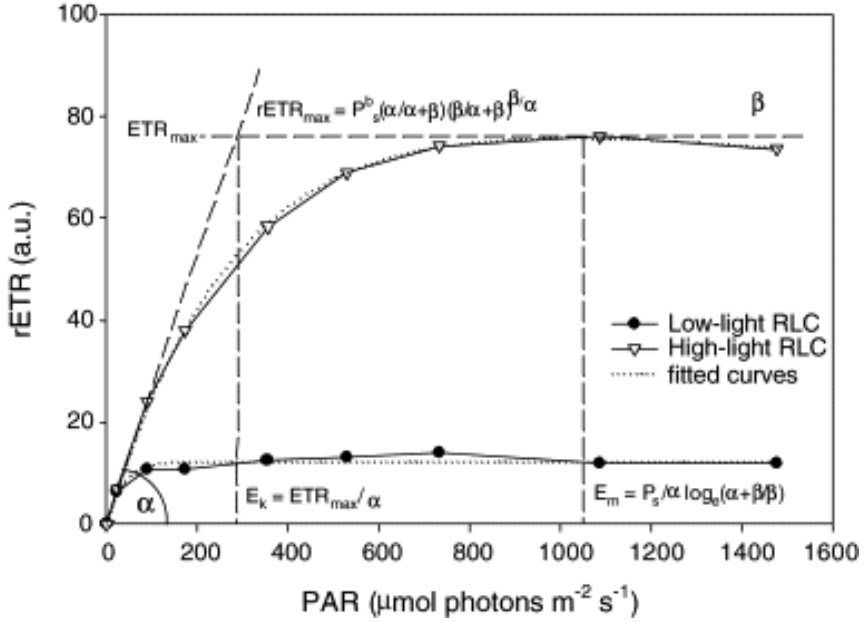

Figure 4: *Basic rapid light curve plot from Ralph & Gademann (2005) with relevant light curve variables labeled. The variables included in my study were α (alpha) - expressed here in arbitrary units (A.U.), $rETR_{max}$ (ps) (µmol electrons $m^{-2}s^{-1}$), and E_k (µmol photons $m^{-2}s^{-1}$). The above plot includes β, the slope when the curve begins to become negative, but that was excluded in this study due to the absence of photoinhibition and all values therefore being 0 (Ralph & Gademann 2005). A similar plot was created for each light curve measurement done with the AquaPen. See Table 3 for definitions of all parameter terms included in this thesis project.*

This curve fitting allowed the calculation of common and useful light curve variable estimates such as the initial slope of the rETR with increasing light intensities (alpha) and the maximum rETR rate (ps). E_k, the photoacclimation parameter, representing the light intensity at which ps would be reached based on alpha, was calculated by dividing ps by alpha (Forget et al., 2007). These, together with the maximum quantum yield (Q_{max}) and F_0 values obtained directly from the AquaPen, were used to assess potential seasonality of photosynthetic performance. F_0 represents the minimum fluorescence while the algae is in a dark-adapted state but is determined when the measuring light at the end of the AquaPen probe is turned on.

***Table 3**: All fitted light curve terms used in this project along with the appropriate units and definitions.*

Term	Units	Definition
α (alpha)	µmol photons $m^{-2}s^{-1}$	Initial slope of relative electron transport rate
rETRmax (ps)	µmol electrons $m^{-2}s^{-1}$	Maximum relative electron transport rate
Ek	µmol photons $m^{-2}s^{-1}$	Light intensity at which ps would be reached based on alpha
F_o	RFU - relative fluorescence units	Minimum chlorophyll fluorescence in dark-adapted state
Qmax	no units - simple fraction (number photons emitted)/(number photons absorber)	Dark acclimated maximum quantum yield

2.6 Calculation of Response Variables and Statistical Analysis

All statistical analysis was performed using RStudio version 4.3.1 (2023-06-16). The Rstudio packages "phytotools" was used to obtain light curve fit results from AquaPen data (Silsbe & Malkin, 2015). The package "lme4" was used to help fit and analyze linear models (Bates et al., 2015), "car" was used to carry out homogeneity of variance testing (Fox & Weisberg, 2019), and "GAD" was used in testing for homogeneity of variances (Sandrini & Camargo, 2023). The package "ggplot2" was used to create and customize plots (Wickham, 2016), and "tidyverse" (Wickham et al., 2019) and "dplyr" (Wickham et al., 2023) were used to transform and manipulate data so that they could be presented more appropriately. The packages "vegan" was used in the multivariate analyses (Oksanen et al., 2022), and "tidyr" (Wickham et al., 2024) and "corrgram" (Wright, 2021) were used to visualize the data more effectively throughout the analyses.

To understand local microalgal biodiversity while considering abundance and evenness of different community groups, Shannon indices were calculated for every sample examined via microscopy. Shannon indices were calculated for these using the major taxa groups and also higher taxonomical resolution groups.

To look at seasonality within the response variables, t-tests were performed on a decreased dataset using only data from the first and last sample day. Using just this data from sampling events on August 31st and December 14th, Welch's independent two sample t-tests were run to compare the alpha, ps, Q_{max}, E_k, F_0, and Chl *a* values between blocks 1 and 2 to test for a block effect. Paired t-tests were run with the same data, just without specifying block, to compare the variables on a temporal scale between the first and last sample dates. The normality assumption for t-tests was tested using the Shapiro-Wilk test (p-value > 0.05), and

homogeneity of variances was tested using Cochran's C test. All assumptions were met for these t-tests.

To further assess seasonality throughout the sample season, two-way mixed ANOVA models were run, including both block and day of the year as independent fixed factors (block as between-groups factor and day of the year as repeated measure factor), for every response variable using the data collected from all the sample days. Initially, the plot number was included in the ANOVA models as a random factor nested within block, but, with the use of the step() function, it was determined the inclusion of plot was not necessary due to it having no significant effect on the response variables. If significant differences were found between groups, a post hoc test (Tukey test) was run as well as Levene's test to determine variance homogeneity, and a significance level of $p < 0.05$ was used. Unfortunately, the assumption of normality amongst the residuals could not be met, despite efforts with data transformation, within ANOVA models for any of the variables. This is important to note due to the possibility of rejecting our null hypothesis when it should not have been rejected.

A Principal Component Analysis (PCA) was performed with the light curve variables (alpha, ps, Q_{max}, E_k, and F_0) to obtain more of an understanding on how these response variables related to each other. A redundancy analysis (RDA) was then performed, using the R packages "vegan," "tidyverse," and "tidyr," to further understand the extent to which the variation amongst the response variables could be explained by the predictor variables. The initial RDA included experimental factors measured. The final RDA model excluded seawater temperature and salinity since they were so highly correlated with plot water temperature and salinity. Creek water temperature was also excluded due to being so highly correlated with the other water temperatures, and air temperature was excluded due to being so similar to sediment temperature. The exclusion of the above variables allowed for a clearer visual model and a more realistic fit result. Therefore, the final RDA included block water temperature, block water salinity, creek salinity, sediment temperature, block, day of the year (included as a relative metric of daylight), and sun elevation angle as predictor variables. The included response variables were alpha, ps, Q_{max}, E_k, and F_0.

3 Results

3.1 Quantitative analysis of microalgal composition and abundance

The average abundance of individual microalgae cells per block varied between the two examined months by about one order of magnitude, with plot 1 in block 2 demonstrating both the highest (157,032 cells cm^{-2}, September) and lowest (11,671 cells cm^{-2}, December) abundances. The average abundance across all samples from both blocks was higher in September with 95,286 ± 39,145 (sd) cells cm^{-2} to 19,600 ± 12,846 (sd) cells cm^{-2} in December. Block 1 samples went from having an average cell abundance of 71,030 ± 31,764 (sd) cells cm^{-2} in September to 20,572 ± 17,688 (sd) cells cm^{-2} in December whereas block 2 samples displayed an average abundance of 119,542 ± 32,506 (sd) cells cm^{-2} in September and 18,626 ± 9,840 (sd) cells cm^{-2} in December. This meant that block 2 had a higher mean abundance than block 1 in September by 68% (48,512 cells cm^{-2}) but a similar abundance to block 1 in December.

Diatoms were consistently the dominant taxa in all samples, ranging from 13,439 cells cm^{-2} (B2P2 in December) to 144,830 cells cm^{-2} (B2P1 in September), and making up 44.3% to 97.9% of the total algal abundances within samples. Block 2 had a higher percentage of diatoms compared with block 1 with mean diatom abundances of 111,761 ± 29,078 (sd) diatoms cm^{-2} (93.9% of total live cells) in September and 17,330 ± 9,627 (sd) diatoms cm^{-2} (92.6% of total live cells) in December. Block 1 had an average of 34,660 ± 11,529 (sd) diatoms cm^{-2} (50.3% of total live cells) in September and 13,086 ± 12,298 (sd) diatoms cm^{-2} (60.0% of total live cells) in December. Colonial cyanobacteria were also major contributors to microalgal abundances, especially in Block 1. An average of 33,481 ± 19,334 (sd) cyanobacteria cells cm^{-2} (45.6% of total live cells) were found in block 1 in September and 3,596 ± 714 (sd) cyanobacteria cells cm^{-2} (24.7% of total live cells) in December. Block 2 contained much less cyanobacteria, with an average of only 707 ± 1,225 (sd) cells cm^{-2} (0.5% of total live cells) in September and 531 ± 176 (sd) cells cm^{-2} (3.5% of total live cells) in December. The amount of unidentified microalgal cells also differed by location and date, but the percentage unable to be identified was at most 14.9% in December block 1 and usually less than 7%. Lastly, relating to size, about half the microalgal cells were less than 50.0µm in length, and about a fourth were typically over 200.0µm. The most common cells represented were pennate diatoms between 10-100µm in length.

a)

b)

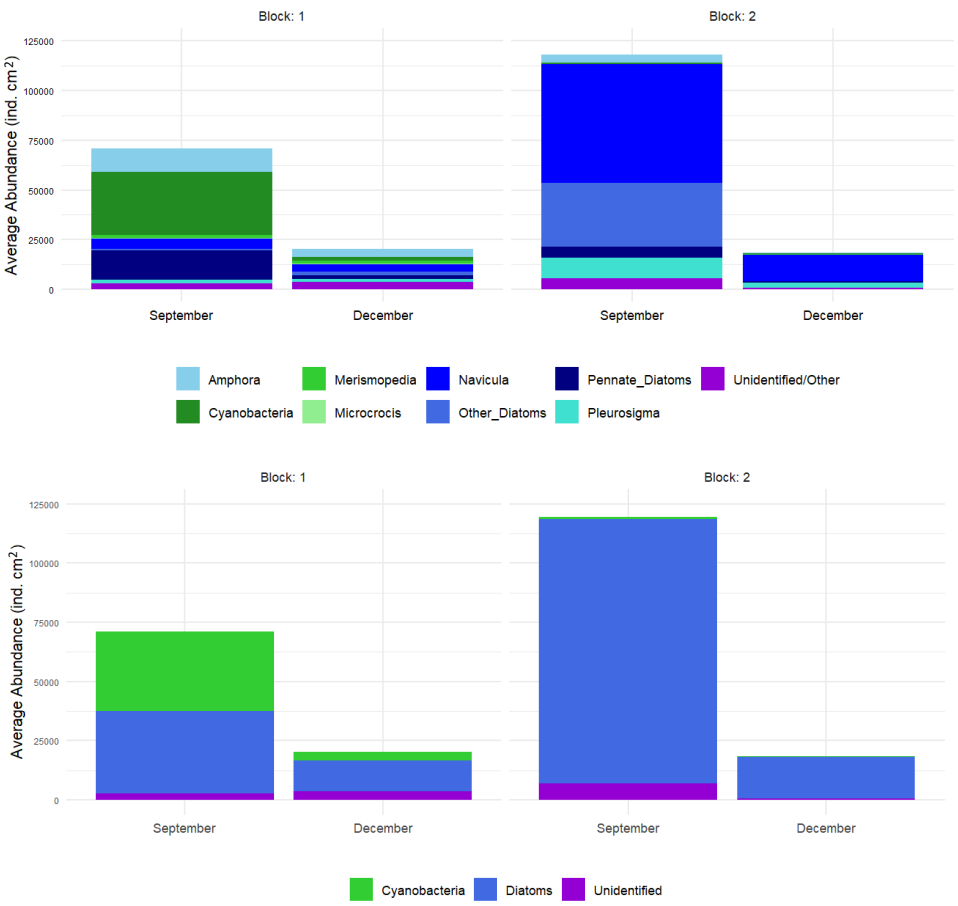

Figure 5: *Abundance of living microalgae in samples from September 20th and December 14th, separated by a) major taxon types, and b) higher taxonomical resolution groups, sorted to the most possible level of identification in most cases.*

Cells which could be identified as microalgal cells, but otherwise indistinguishable due to orientation or other reasons, were counted into an "unidentified" category during microscopy lab work. It should also be noted that the presence and abundance of sponge spicules (not counted in cell count data) increased considerably from the September to the December samples, especially in block 1 which went from having close to none per sample in September to several hundred per sample in December.

Looking more specifically at identifiable taxa, the most common cyanobacteria genera were primarily *Merismopedia* and *Microcrocis* (Figure 5b). Identifiable diatom genera included *Navicula*, *Amphora*, and *Pleurosigma*. There were unfortunately many pennate diatoms visible in samples which could not be clearly and confidently identified using light microscopy and were counted as "pennate diatoms." Diatoms placed in the "other diatoms" category were a mix of centric diatoms and diatoms which were difficult to distinguish by shape.

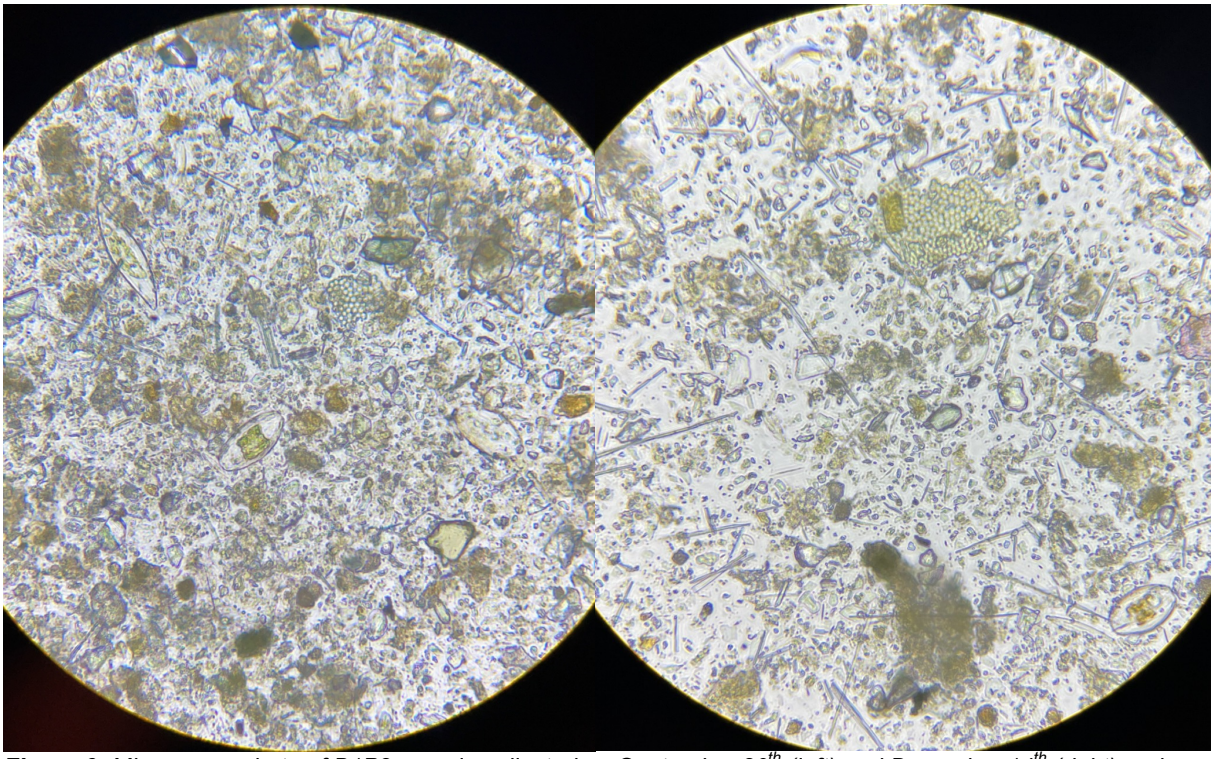

Figure 6: *Microscopy photo of B1P2 sample collected on September 20th (left) and December 14th (right) and analyzed in the lab on January 24th and March 12th, 2024.*

Month	Block	Plot	Shannon Index
September	1	1	1.40303
September	1	2	1.63366
September	1	3	1.60299
September	2	1	1.28541
September	2	2	0.94573
September	2	3	1.21879
December	1	1	1.87928
December	1	2	1.82449
December	1	3	1.96534
December	2	1	1.33783
December	2	2	0.76655
December	2	3	0.90427

There was an increase in Shannon index values in all the plots in block 1 and in plot 1 of block 2 from September 20th to December 14th. Shannon indices ranged from 0.79 to 1.97 in the twelve sediment samples looked at during microscopy work. Results from a Welch's two sample t-test run on the Shannon indices from September and December determined that there was no significant difference between the two months' sample Shannon indices ($t(7.3) = -0.41$, $p = 0.6923$).

Table 4: *Calculated Shannon diversity indices for sorted microalgae groups identified through microscopy.*

3.2 Pigment concentration (Chl *a*)

The sediment Chl *a* concentrations ranged from 0.05-17.98µg Chl a cm^{-2} throughout the sample season. The averages per month were as follows: 8.00µg Chl *a* cm^{-2} in August, 4.81 µg Chl *a* cm^{-2} in September, 9.06µg Chl *a* cm^{-2} in October, 8.73µg Chl *a* cm^{-2} in November,

and 4.71µg Chl *a* cm^{-2} in December. As seen in Figure 8, the Chl *a* values from block 1 and block 2 were not always in the same range, and neither block was consistently lower or higher in average value than the other for any given sample day. However, samples from both blocks displayed a similar decrease towards the end of September, followed by an increase throughout October, and then a stronger decrease until the final sample day on December 14th.

Looking first at Chl *a* concentration analysis, the results from the paired t-test revealed a significant difference ($t(5)=4.15$, $p=0.00884$) in mean concentration of Chl *a* by date, meaning between the samples collected on August 31st and those collected on December 14th. The results from the Welch's independent two samples t-test, however, concluded that there was no significant difference ($t(8.60)=1.25$, $p=0.24$) between the mean Chl *a* values in block 1 versus block 2, again using the data just from the first and last sample day. From the two-way ANOVA, using all Chl *a* data from the entire sample season, the only predictor variable with a significant effect was the day of the year ($p=0.049$). Amongst the biological variables from the AquaPen data, t-tests revealed no significant difference (p-values > 0.05) between the blocks, again using just the data from the first and last sampling day. There was a significant difference between the first and last sampling events for variables alpha, ps, Q_{max}, and E_k (p-values < 0.05). For complete results from these t-tests and ANOVAs, see Figure 5, Figure 6, and Appendix.

3.3 Photophysiological variables

Seasonal changes in the photosynthetic performance were seen in both blocks. Examples of the data resulting from the rapid response curve measurements are provided in Figure (Results 3). The values for alpha changed by one order of magnitude and ranged from 0.05 to 0.53 throughout the sample season with most averages between 0.15-0.45. Alpha values overall increased from August 31st to September 29th, then entered a stationary phase through November 15th, and showed a brief second peak in values on November 21st before having an overall decrease into the end of the sample season. The estimated maximum rETR rate (ps) ranged from 3.42 to 353.81 throughout the sample season, but most data were between 10-200. E_k, which represents the light intensity ps would be reached based on alpha, ranged from 17.8 to 3101.0 with most values between 30-800. The variables ps and E_k both displayed an opposite pattern to alpha with an initial decrease into the beginning of September, an increase on October 16th, and then with an overall decrease heading towards December 14th. The dark acclimated maximum quantum yield Q_{max}, which ranged from 0.00 to 0.77, displayed an overall increase throughout the sample season but with a relatively stationary period from October 16th to November 6th. Q_{max} also contained more outliers than any of the other variables. F_0, representing Chl *a* initial fluorescence of dark acclimated samples, had a seasonal range of 0 to 63916, and decreased from August 31st to December 14th. Block 1 had slightly higher average values on August 31st but otherwise remained mostly below 2000 with averages decreasing to below 500 from November 10. Block 2, on the other hand, increased to a peak in September before gradually decreasing towards December 14th with a sudden spike in values just on November 1st.

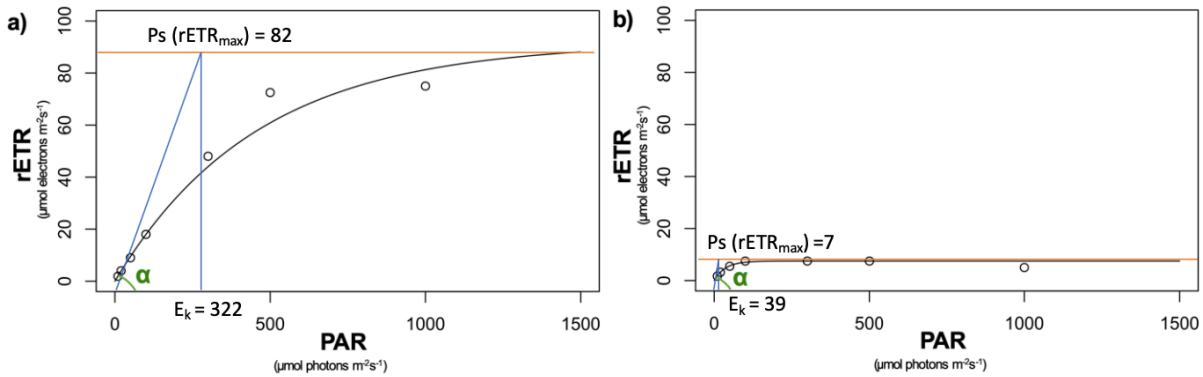

Figure 7: *Rapid light response curves for light curve 3 (LC3) measurements taken from plot 1 in block 1 with AquaPen on a) August 31st and b) December 14th, 2023, with light curve variable estimates alpha, ps, and E_k labeled. The alpha value was 0.25 on August 31st and 0.17 on December 14th.*

a)

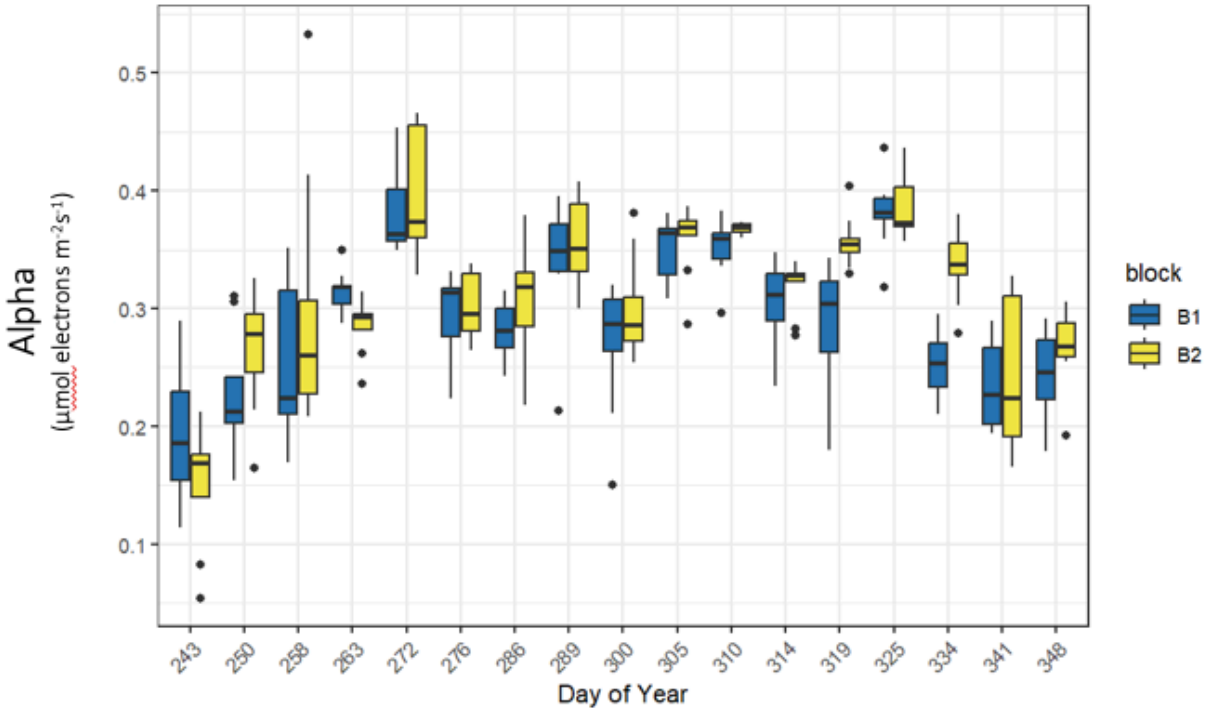
Alpha
(µmol electrons m⁻²s⁻¹)
0.5
0.4
0.3
0.2
0.1
243
250
258
263
272
276
286
289
300
305
310
314
319
325
334
341
348
Day of Year
block
B1
B2

b)

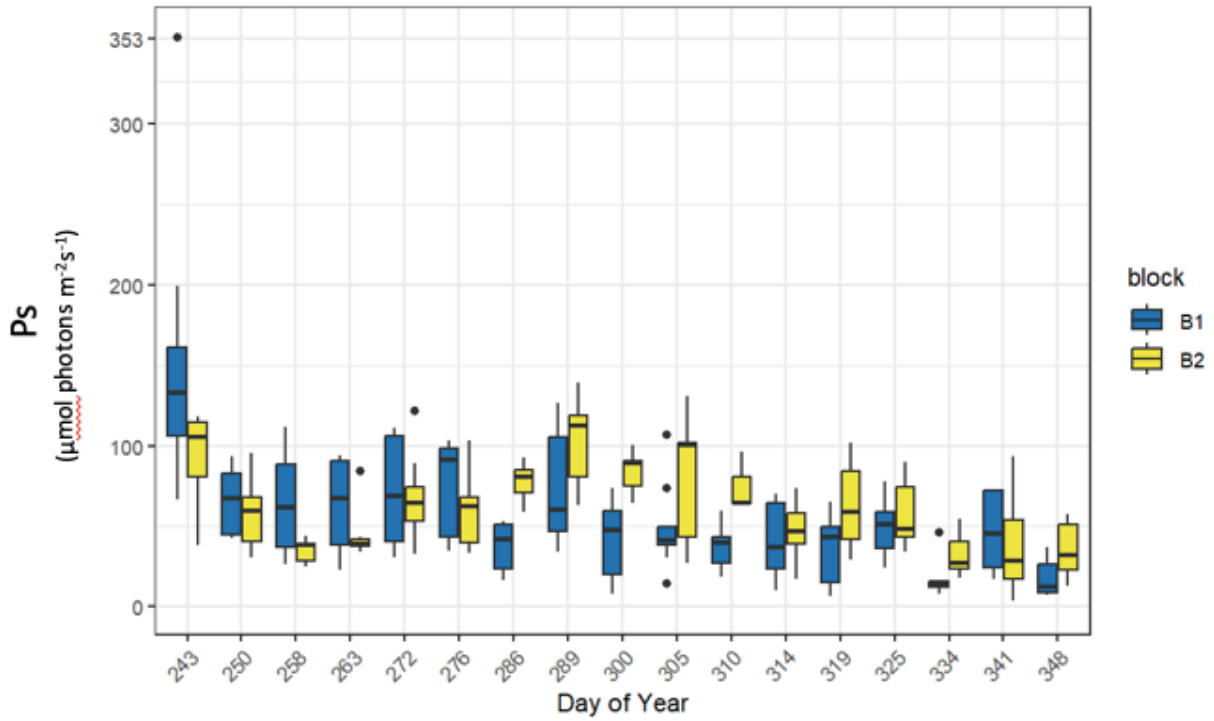
Ps
(µmol photons m⁻²s⁻¹)
353
300
200
100
0
243
250
258
263
272
276
286
289
300
305
310
314
319
325
334
341
348
Day of Year
block
B1
B2

c)

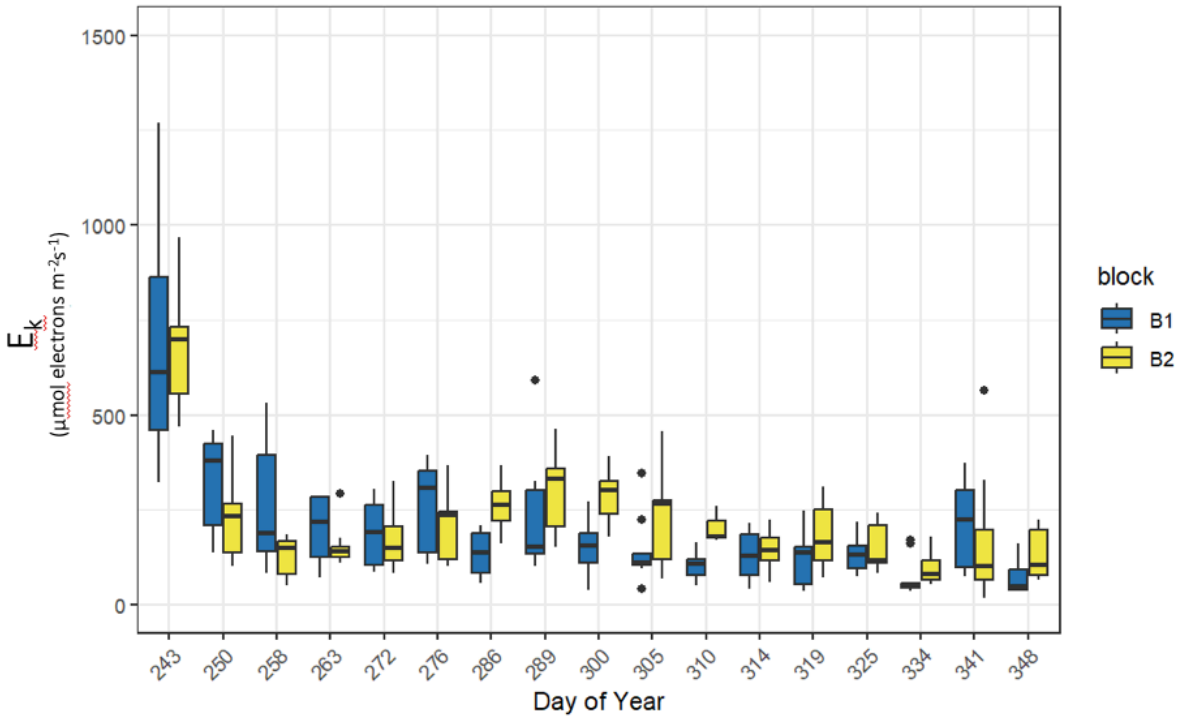
1500
1000
500
0
E_k
(µmol electrons $m^{-2}s^{-1}$)
243
250
258
263
272
276
286
289
300
305
310
314
319
325
334
341
348
Day of Year
block
B1
B2

d)

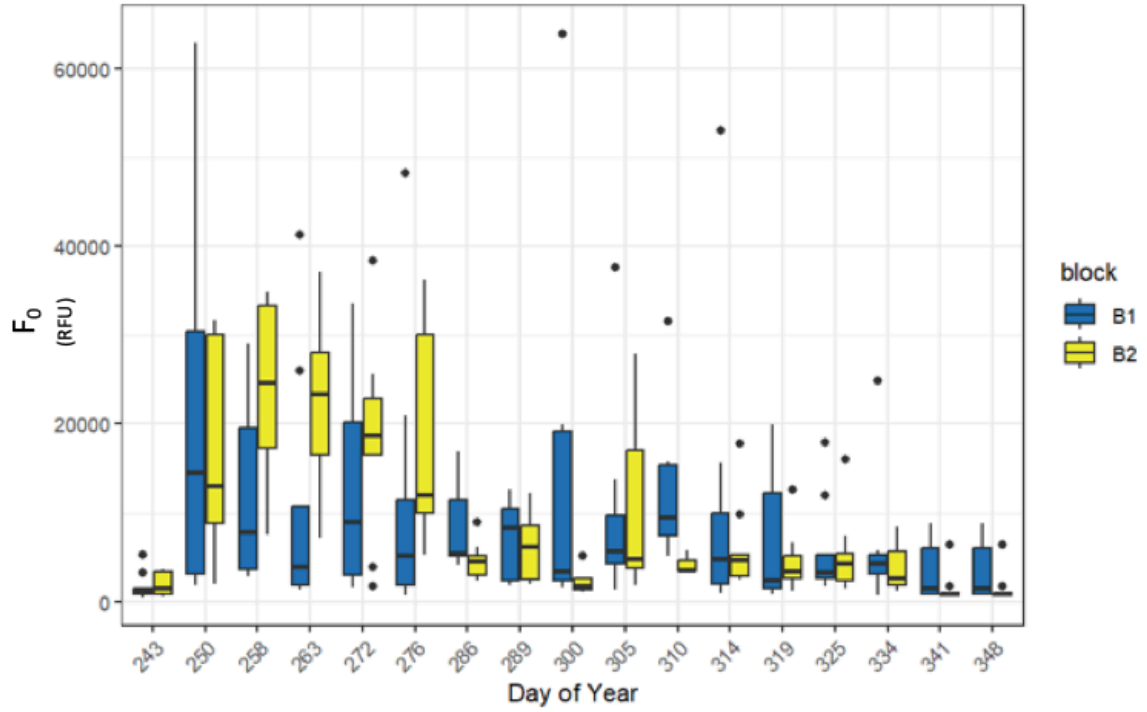
60000
40000
20000
0
F_0
(RFU)
243
250
258
263
272
276
286
289
300
305
310
314
319
325
334
341
348
Day of Year
block
B1
B2

e)

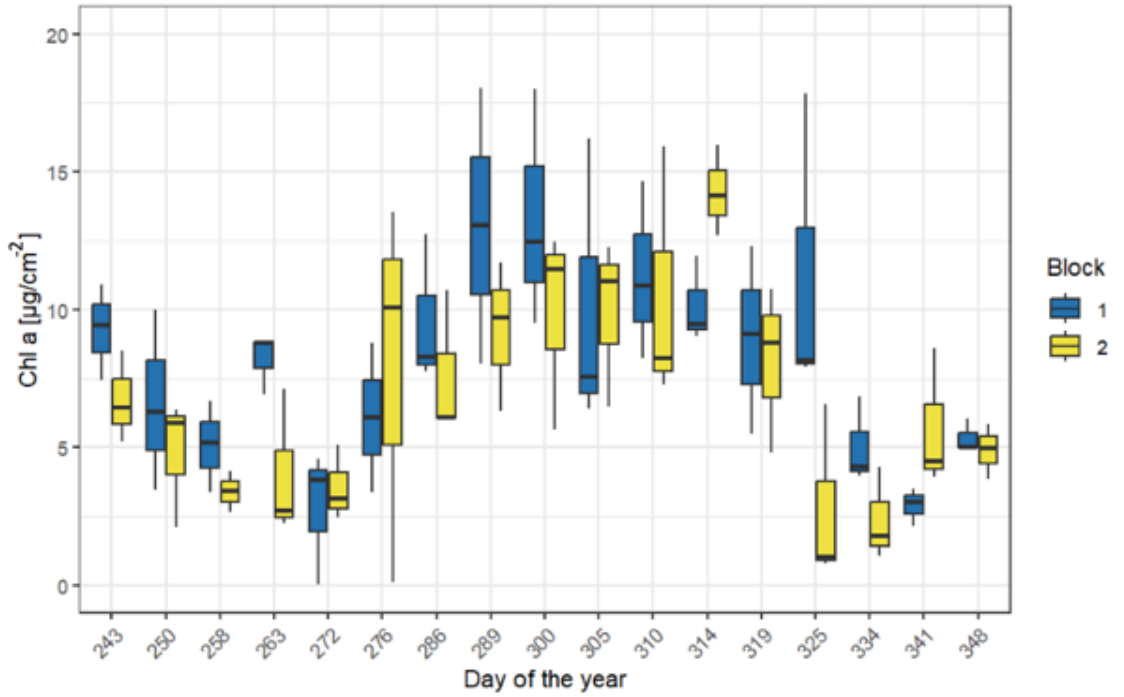

f)

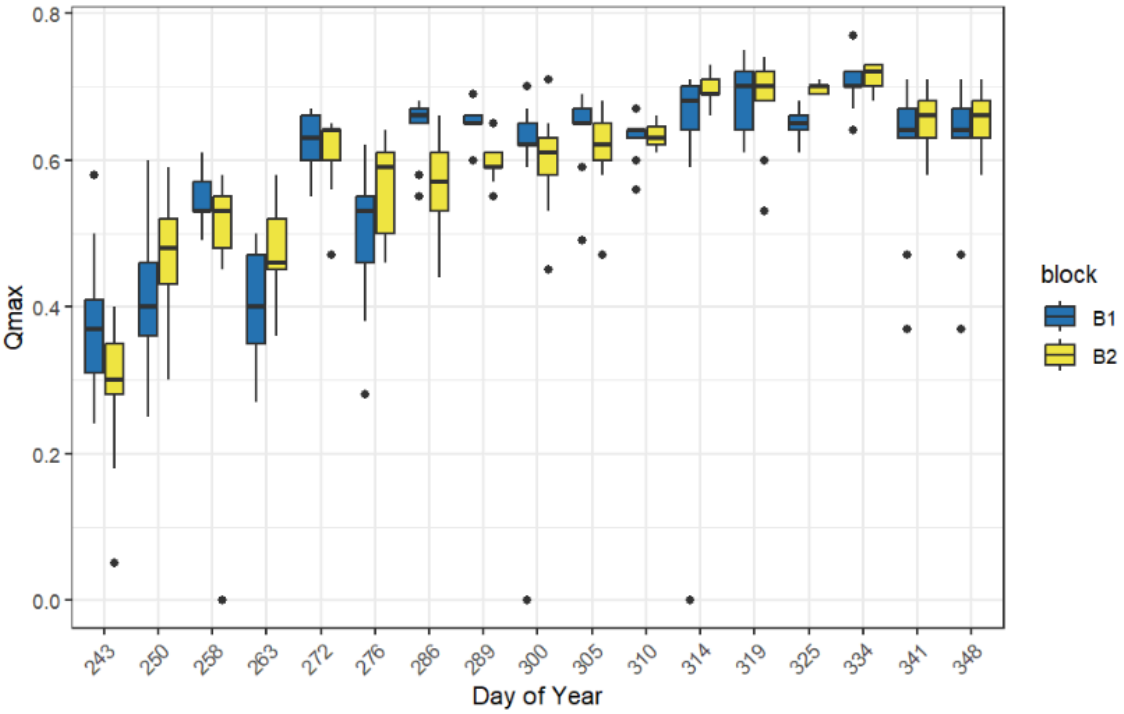

Figure 8: *Light curve response variable measurements from each weekly sample day plotted on the day of the year(DOY) samples were taken and separated by block. (a)Alpha (µmol photons $m^{-2}s^{-1}$) throughout season in block 1 and 2. (b) ps (µmol electrons $m^{-2}s^{-1}$) throughout the season in block 1and 2. (c) E_k (µmol photons $m^{-2}s^{-1}$) throughout season in block 1 and 2 (note that one outlier with a value of 3101.00 on day 243 is not shown in the plot). (d) F_0 (RFU) throughout season in block 1 and 2. (e) Chl a (µg/cm^2) throughout season in block 1 and 2. (f) Q_{max} throughout season in block 1 and 2*

Table 5: *Summary of t-tests run to analyze significant effects of the block and sample date among the biological response variables. Headers are the number of sample size (n), standard deviation (SD), degrees of freedom (df), and p-value.*

Dependent variable	Grouped by	n (per each block or day)	Mean	SD	df	p-value
Chl *a* (µg/L)	Block	6	Block 1=51.693 Block 2=41.134	Block 1=17.219 Block 2=41.134	8.608	0.242
	Sample day	6	August=56.583 December=36.244	August=14.542 December=5.492	5	0.00884
alpha (µmol photons $m^{-2}s^{-1}$)	Block	18	Block1=0.217 Block 2=0.210	Block 1=0.0538 Block 2=0.0742	31.007	0.769
	Sample day	18	August=0.171 December=0.256	August=0.057 December=0.036	17	7.12E-05
ps (µmol electrons $m^{-2}s^{-1}$)	Block	18	Block1=85.102 Block2=65.458	Block 1=91.340 Block 2=36.933	22.414	0.4066
	Sample day	18	August=123.803 December=26.757	August=68.221 December=16.471	17	3.23E-05
Qmax	Block	18	Block 1=0.493 Block 2=0.468	Block 1=0.159 Block 2=0.208	31.733	0.688
	Sample day	18	August=0.33 December=0.632	August=0.115 December=0.0866	17	1.36E-06
Ek (µmol photons $m^{-2}s^{-1}$)	Block	18	Block 1=511.0193 December=396.960	Block 1=742.961 Block 2=293.735	22.188	0.551
	Sample day	18	August=805.0456 December=102.934	August=616.696 December=62.165	17	0.000208
F_o (RFU)	Block	18	Block 1=2578.333 Block 2=1712.000	Block 1=2624.092 Block 2=1527.342	27.333	0.2364
	Sample day	18	August=1816.111 December=2474.222	August=1352.12 December=2749.263	17	0.409

Results from two-way ANOVAs, performed to analyze the effect of block and day of the year on all the biological variables, revealed that there was a statistically significant interaction between block and day of the year among variables alpha and F_0. Simple main effects analysis revealed that block and day of the year separately had a significant effect on alpha values and that the day of the year alone had a significant effect on variables ps, Q_{max}, E_k, F_0, and Chl *a* throughout the sample season (see Table 6 for relevant statistical values).

Table 6: *Summary of two-way ANOVA, showing only the predictor variables with p-values <0.05, for biological response variables. Headers are sum of squares (SS), degrees of freedom (df), mean squares (MS), F value (F), and p-value. See Appendix Figure 2 for complete table, including variables with insignificant results (p-value>0.05).*

Dependent (response) variable	Significant source of variance	SS	df	MS	F	p-value
Chl *a* (µg/cm^{-2})	Day of year	67.2	1	67.23	4.02	0.049
	Residuals	1070.3	64	16.72		
alpha (µmol photons $m^{-2}s^{-1}$)	Block	0.032	1	0.03202	16.234	7.32E-05
	Day of year	0.8792	16	0.05495	27.856	<2e-16
	Block x Day of year	0.0664	16	0.00415	2.103	0.0086
	Residuals	0.5227	265	0.00197		
ps (µmol electrons $m^{-2}s^{-1}$)	Day of year	166007	16	10375	2.647	0.00067
	Residuals	1105499	282	3920		
Qmax	Day of year	2.915	16	0.18219	21.61	<2e-16
	Residuals	2.385	283	0.00843		
Ek (µmol photons $m^{-2}s^{-1}$)	Day of year	7922170	16	495136	6.094	1.50E-11
	Residuals	22910628	282	81243		
F_o (RFU)	Day of year	8.58E+09	16	535978619	6.077	2.08E-11
	Block x Day of year	2.74E+09	16	171205436	1.941	0.0173
	Residuals	2.35E+10	266	88202741		

3.4 Multivariate Analyses

The overall RDA was significant (df=7, variance=1.274, F=12.618, p= 0.001) along with the first two axis (p-values (both) = 0.001). The first two axis combined explained 22.9 % of variance in the response variables (RDA1: 16.5%, RDA2: 6.5%,). Among the explanatory variables, the ones which were determined as significant were day of the year (p-value = 0.001), sediment temperature (p-value = 0.010), water temperature (p-value = 0.001), water salinity (p-value = 0.001), and creek salinity (p-value = 0.004). As seen in Figure (Results figure 5) from the variation in arrow length, block and water salinity had much less strength compared to water and sediment temperature, sun angle, and day of the year.

Looking at the RDA plot (Figure 9), we can see that the sun elevation angle, sediment temperature, and water temperature were correlated and had a positive relationship but that water salinity, creek salinity, block, and day of the year were not particularly correlated to other predictor variables. Day of the year was however a highly influential variable and negatively correlated to sun angle and temperature.

Focusing on the response variables though, alpha has a negative relationship with E_k and ps, telling us that when the initial rate of the rETR was higher, the algal cells had a lower maximum rETR rate and required a higher irradiance to reach that maximum level. All the measurements from August are characterized as having these higher E_k and ps values. Figure 8 highlights this as we can see higher E_k and ps values with lower alpha values from the sampling event in August. November points are in the vicinity of the August ones, although they are slightly less strongly correlated with E_k and ps. Within the October points is where we can see a shift to higher correlation with alpha, pointing to an increase in alpha values and decrease in E_k and ps. November and December points display a considerable amount of variation but are slightly more clustered around the response variables F_0 and alpha. Although water salinity and creek salinity had less strong of an effect compared to other predictor variables, F_0 had a distinct negative relationship with water salinity, and E_k and ps had a negative relationship with creek salinity.

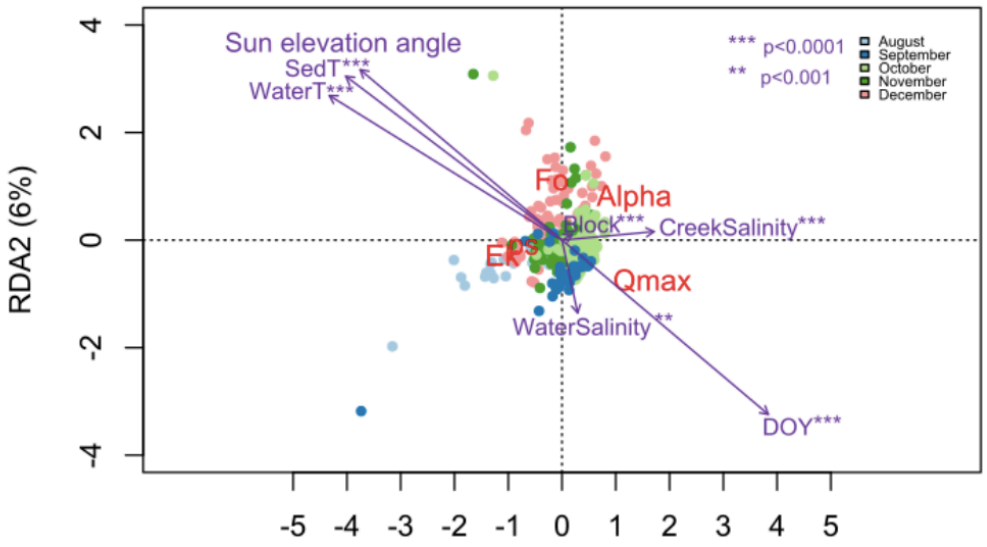

Figure 9: *Redundancy Analysis performed on the light curve parameter variables (response variables) taken from throughout the entire sample season and selected predictor variables. Each point represents a light curve measurement taken by the AquaPen in the field, and each color represents measurements from a different calendar month (August-December).*

An additional RDA model and plot was created using a subset of the data in order to be able to include Chl *a* concentrations as a biological response variable. The overall model was significant (df=6, variance=1.455, F=3.8961, p=0.001), and the first two axes also explained 22% of the variance in the response variables (RDA1: 16%, RDA2: 6%). However, only RDA1 was significant (RDA1 p=0.001, RDA2 p=0.217). The only significant environmental variable was creek salinity (p=0.047). The previously included biological response variables had similar relationships with each other and with the environmental variables as in Figure 9. With the addition of Chl *a*, there is a negative relationship demonstrated with alpha, F_0, creek salinity, and the distribution points to higher Chl *a* values in December and lower values in September. This temporal variation is also demonstrated in Figure 8. The RDA plot including Chl *a* is included in Figure 5 of the appendix at the end of this thesis.

4 Discussion

4.1 Summary of main findings

This thesis project evaluated for the first time seasonal aspects within microphytobenthos (MPB) communities in an intertidal zone on the island of Tromsøya. The results suggest seasonal changes in benthic microalgal community abundance, composition, and photophysiology. Overall mean live cell abundance decreased in December to at least a third of what it was in September, and the make-up of the samples shifted to a higher percentage of diatoms from September to December. There were clear seasonal changes in values of photophysiological responses and algal Chl *a* concentrations throughout the sample season. As the seasonal weather conditions changed, there was evidence of continued algal activity, with a higher Q_{max} value in December than August, and similar alpha values on the last sample day to the first one. Although some variation was present between the two sample blocks, they both demonstrated very similar seasonal photophysiological variable and Chl *a* concentration responses despite the differing proximity to freshwater outflow and surrounding macroalgae taxa. In the following discussion, I will first focus on methodological challenges related to this field study, followed by examining the seasonal variability of algal physiology and diversity, and ending with a conclusion with an outlook for further studies.

4.2 Methodological Challenges

The basic nature of my sampling location and schedule brought many challenges, both predictable and unexpected. The air temperatures at beginning of the sample season exceeded 10˚C on the first couple sample days while later in the season cold temperatures, rain, snow, ice, and fog made sampling challenging. Due to the timing of the tides and the seasonal variation of local weather conditions, it just was not possible to only sample in the same conditions. Ice and snow covering the plots did affect the distance from which the AquaPen sensor could be from the sediment surface. Based off of qualitative field data and observations, I could not see any clear correlation between precipitation or presence of ice/snow with resulting response variable values though. As seen in Figure (results 4), there was significant variation in alpha and E_k values on December 7th, the day with the most ice and snow covering plots, but there was also significant variation in September when there were no obstacles potentially blocking the sediment surface. When the snow covered an area, I would scrape off the top layer of snow until I managed to expose a relatively transparent level of ice on top of the sediment. I never scraped all the snow or ice off the surface because I did not want to scrape off algae. Stronger windy conditions occasionally tipped the AquaPen over for a few seconds before I could stand it back up. Fortunately, there were no technical failures due to weather conditions.

In the beginning of the sample season, plots had not been affected by my walking paths around them to take measurements with the AquaPen, and the sediment surface had been less disturbed from the placement of the square plot marker and pots used to provide a dark environment for the algae. However, the marks left behind by my footprints and the pots were sometimes visible for weeks throughout the sample season, see Figure (discussion 1). The location where the AquaPen sensor would measure was never on these marks, and sampling

near these marks from a previous week did not show any effect in the data, but disturbances cannot be excluded. Similarly, the metal rods used to mark two of the plot corners had the potential to affect the surrounding sediment throughout rust erosion. However micro-nutrient limitation can be excluded for coastal intertidal sites due to the high input of land-based iron entering the coastal marine systems around Tromsø mainly through weathering (Höper et al., 2022, Flaten 1991). There was also evidence of other activity affecting the sediment surface while I was away from the site. I found fresh human boot prints in the middle of a plot one day, but usually marks were likely from local wildlife. More than once, I found bird prints in my plots, and one time I saw a couple otters running through block 2, one of them running directly through one of my plots. Furthermore, I had no way of knowing how these areas of sediment were affected in ways that did not leave visible markings for me to see while doing fieldwork. Activity in the nearby bodies of water, such as boat traffic, could have also chemically altered environmental conditions for the microalgae. However, the natural disturbances will result in realistic scenarios, as all sites will experience these.

Figure 10: *Photo taken from fieldwork on September 7th of plot 3 in block 1 with visible pot marks remaining from a previous sampling event.*

Apart from environmental factors challenging the consistency and ease of my sampling, my own procedures introduced some inconsistency due to me making small adjustments as I discovered which protocols worked best. For the photosynthetic yield measurements, it is important to expose the samples to complete darkness for at least five minutes. I started the sample season using dark painted thick plastic plant pots with a wide lip for this purpose. The pots were shedding increasingly more and more dry paint with every sample day, and the wide lip left extremely destructive rings in the sediment. I switched to using empty yogurt cups covered in thick layers of duct tape on October 13th because they were less destructive and did not leave behind dry paint flakes. Ideally, the switch to a more effective tool would have been made before I started the sampling for the season, but I did what I could to limit the extent to which changes in methodology could have altered results. Furthermore, it was the first study of this kind at UiT, so a lot of learning occurred during sampling.

Lastly, a challenge for the microscopic analysis was the presence of a considerable amount of debris, which included mineral grains and empty diatom frustules in the samples. The presence and number of sponge spicules also became quite abundant in the December samples, potentially due to the fact that diatoms attached to siliceous sponge spicules (Gómez et al., 2009). This amount of inorganic material made identifying all cells in the microscopic approach difficult. The dilution procedure used was helpful in decreasing the amount of debris, but it will remain an intrinsic problem for sediment living microalgal diversity analysis.

4.3 Seasonality in composition and abundance

The seasonal range of air temperatures from August to December 2023 in Tromsø were close to the averages from the previous three years, fluctuating mostly between 4˚C and 10˚C in September and –2˚C and -9˚C in December (seklima.met.no, 2023). Therefore, we can use the weather and field condition data as representative for a typical transition season into winter for Tromsøya.

4.3.1 Abundance and composition through microscopy

Through microscopy, community composition and abundance were assessed by counting live cells and identification of the lowest possible taxa, when possible, in sediment samples taken from September 20th and December 14th.

The clear differences, both in composition and abundance, between the September and December algal communities demonstrate a seasonal change in the communities. Overall abundances based on cell counts, from both September and December, were comparable to data from other Arctic and sub-Arctic microphytobenthos (MPB) studies. Some examples of sub-arctic intertidal and littoral subtidal microphytobenthic abundance estimates are $12.4x10^4$–$14.8x10^4$ cells cm^{-2} (Trondheimsfjord, Norway), $0.25x10^6$–$2.1x10^6$ cells cm^{-2} (Laholm Bay, Sweden), and $4.7x10^6$–$7.5x10^6$ cells cm^{-2} (Gulf of Finland) (Taasen and Høisæter (1981), Sundbäck and Jönsson (1988), and Snoeijs (1990)).

Expectations from previous studies have predicted an increase in temperature leads to an increase in fast-growing dominant diatom species, thus leading to a decrease in community diversity, but results have not supported a clear relationship between temperature and diatom percent cover (Snoejis 1990). The results from this study do not support a hypothesis that predicts lower community diversity with higher temperatures either. While some of the lower Shannon indices were seen in December, when compared to September, there was not a significant difference between the Shannon indices between the two months, which had average fieldwork air temperatures of 7.82˚C (sd= 0.53) and –3.63 (sd= 0.09).

The high percentage and often dominance of diatoms throughout the sampling period aligns with other MPB study results, both from the Arctic and other areas of the world (Malakhov 2021, Scholz & Einarsson 2015). In Trondheimsfjord, diatoms comprised 87% of the total biomass, and in Arctic sub-tidal flat communities have in fact consisted of up to 99% diatoms (Cibic et al., 2007 &Woelfel et al., 2009). In northeast Greenland, diatom biomass has

contributed 24-96% of intertidal MPB, and off the coast of the White Sea diatoms can make 80% of the total abundance in the middle intertidal zone (Stumm & Berninger 2005, Azovsky et al. 2013). Even in Svalbard, the MPB is dominated by diatoms, including *Navicula, Amphora,* and *Pleurosigma* which were found in this study (Sevilgen et al., 2014). *Navicula*, one of the most common diatoms in my samples, is also a prevalent taxon in other sub-Arctic and Arctic microphytobenthic communities on intertidal flats, often considered a key taxon in intertidal mudflats (Scholz & Einarsson 2015). Other diatoms, such as *Pleurosigma* and *Amphora,* have also been notable taxa found in sub-arctic areas of Norway and Sweden (Cibic et al., 2007, Sundbäck and Jönsson 1988).

Cyanobacterial abundances were higher at block 1, which was located further away from the freshwater creek compared to block 2. Scholz et al. (2012) found a distribution of cyanobacteria with highest abundances in the seaward ends of their transects, which could be for a similar reason as to why the cyanobacteria abundances were further away from freshwater in this study. Another potential reason could be the variation in depth of the water pools forming on the sediment surface. Benthic diatoms are often able to inhabit areas in deeper water and outcompete cyanobacteria in cold low-light environments because they have, on average, a lower E_k, which allows them to inhabit areas with lower light intensity (Gómez et al., 2009). This was not likely at my site, as no extensive pools were seen at low tide. However, the presence of occasional snow and ice in the plots could have presented a similar effect.

From September to December, the significant shift to lower percentage of cyanobacteria in block 1 could be a seasonality effect. Similar decreases of cyanobacterial contributions were seen in other studies. For example, studies further south in the northern hemisphere in Chesapeake Bay have reported more mixed MPB community structures in summer and fall compared to a higher percentage of diatoms in winter and spring (Semcheski et al., 2016). Even in Greenland cyanobacteria are known to peak in the summer months (Stumm & Berninger 2005). In southern Sweden, diatoms such as N*avicula* and *Melosira* have been favored in the earlier months of the year which host more wintery weather conditions (Snoeijs 1990).

Possible reasons for a composition shift throughout the sample season include seasonal weather changes creating a colder and darker environment in which the microalga are less productive, as seen in the lower algal abundances in December. However, algae were still present at the time even in December when they also still showed high growth potential as seen in the photosynthetic yield. There is evidence to suggest that certain microalga have developed survival mechanisms to acclimate to otherwise harsh conditions. Many polar and arctic algae have metabolic strategies for cold adaptation, including the maintenance of fluid biological membranes through unsaturated fatty acids within cell membranes, the evolution of antifreeze proteins, and adaptations of the photosynthetic electron transport chain allowing them to complete their life cycles and photosynthesize in temperatures near 0˚C (Gómez et al., 2009). Pennate diatoms, of which there were many in this study, can very efficiently adjust their photosynthetic activity to current radiation condition in polar regions (Gómez et al., 2009).

In further support of the shift to higher percentage diatoms later in the sample season, certain diatom species, such as *Navicula* and *Amphora,* which were both found in all samples for this project, can express a high level of versatility in physiology through heterotrophy (Admiraal & Peletier, 1979 and Cooksey & Chansang, 1976). Heterotrophic utilization of organic

substances by diatoms is a survival strategy used when light levels are too low for photosynthesis and can be specifically important during the polar night conditions (Cibic et al., 2007, Johnsen et al. 2020). *Navicula* species from Svalbard have been specifically studied, leading to knowledge that these benthic diatoms use stored lipid compound triacylglycerol (TAG) and free fatty acids (FFA) during the polar night (Johnson et al., 2020).

Had there been time to perform microscopy on samples from all the months where sampling occurred, we could have obtained a more inclusive look into the composition changes throughout the season. However, we only have microscopy results from one day in September and one day in December. The extent to which samples from these two days represent different seasons is debatable and should be questioned, due to not only the lack of samples from other days in those time periods but also the variation that exists in the definition of a season. Some studies differentiate the seasons of summer and winter in Tromsø by the light and dark conditions, thus defining winter as November, December, and January (Hall et al., 2007). The average air temperature from fieldwork data in September was 9.0˚C (sd=2.9) with green leaves remaining on deciduous plants whereas the average air temperature from December sampling events was –3.2˚C (sd=0.4) with leafless trees and snow covering the ground. Given the change both in light and weather conditions, the samples from September and December are therefore considered to be representative of different seasons.

4.3.2 Abundance through chlorophyll *a* concentrations

Interestingly, the range and variability of mean Chl *a* concentrations can be compared to data found in much warmer places, such as Spain where a range of 6-18µg Chl cm^{-2} *a* was found, although overall there is a trend for arctic areas to have lower Chl *a* concentrations compared to lower latitudes (Varela & Penas 1985, Stumm & Berninger 2005). Compared to springtime Chl *a* values from Svalbard, levels from this study were slightly higher but still comparable and near the same range (Leu et al., 2006). As demonstrated in other European areas such as Germany, benthic Chl *a* values are often expected to be high in the summer and low in the winter (Scholz et al., 2012). However, studies on MPB in Germany also observed an October peak (Stumm & Berninger 2005) similar to this study's peak around day 300 (October 27th). One potential cause for this could be a late autumn bloom, as also oserved for phytoplankton, especially since these biomass peaks in the northern hemisphere tend to be shorter in duration and occur later in the year with increasing latitude (Macintyre et al., 1996). Unfortunately, inorganic nutrient concentrations were not available for this study, but it can be expected that values in the autumn increased and contributed to increased biomass of MPB (Sundbäck et al., 2004).

As a final note relating to Chl *a* measurements, it should be noted here that Chl *a* analysis does not measure only chlorophyll from microalgae and can be biased from the added effects from macrobenthic vegetation and terrestrial plant detritus (Cibic et al., 2007). This could always be a reason for obtaining Chl *a* levels higher than what might be expected and highlights the value of including microscopic analyses to study the presence of microalgae in samples.

4.4 Photophysiology

The variable fluorescence measurements provided a more detailed insight into the photophysiology of the microphytobenthos (MPB) on Tromsøya. Light curve variables were comparable to in other polar locations, highlighting the potential similarities between the ecosystems and their functioning. The range of E_k values after the first sample day aligns with E_k values from late summer in Brown Bay, Antarctica (Salleh & McMinn 2011). However, E_k values were higher, and alpha values all lower, in this study when compared to intertidal microphytobenthos communities in Portugal, suggesting potentially very different ratios between the variable estimates in polar regions versus other regions (Cartaxana et al., 2015).

Q_{max} values largely increased throughout the sample season, despite the decrease in necessary sunlight for photosynthesis, and there was in fact a quite strongly negative relationship between Q_{max} and the sun angle according to the RDA plot in Figure (Results 5). Less sun exposure and less direct sunlight due to both seasonality and the sunlight being blocked by mountains may decrease the likelihood of photodamage, thus leading to higher Q_{max} values. Therefore, Q_{max} may have increased with decreasing light in order to reduce photodamage. However, some studies suggest that benthic microalgal communities rarely exhibit photoinhibition or photodamage due to the downward migration capabilities of diatoms (Woelfel et al., 2014). For example, in the Antarctic summer benthic microalgae exposed to 450 µmol photons $m^{-2}s^{-1}$ did not experience any photosynthetic damage or irreversible photoinhibition (Salleh & McMinn 2011). Alternatively, the likely higher inorganic nutrient concentrations can sustain higher Q_{max} values towards December. However, one should remember that Q_{max} values do not provide direct primary productivity information but are considered a value indicating growth potential.

There was a negative relationship between days of the year and sediment and water temperatures in the RDA plot, indicating the seasonal cooling of the samples. The response variables alpha and F_0 demonstrated a slight positive relationship with sediment and air temperature, especially in the second half of the sample season, whereas Q_{max} had quite a negative relationship with sediment and air temperature (see Figure 9). The RDA plot along with Figure 8 further demonstrate this relatively negative relationship between F_0 and Q_{max} which fluctuates throughout the sample season. Variables E_k and ps had a weaker, albeit positive, relationship with temperature (both air and sediment temperatures). The fact that we see this switch to a lower alpha and higher E_k and ps later in the year suggests a seasonal effect, and this argument is strengthened by the fact that both the RDA model and day of the year from the ANOVA results are highly significant ($p<0.005$).

Similar investigations on Antarctic benthic algae using rapid light curves at similar light levels revealed that alpha had a slightly negative relationship with surrounding temperatures, but the variables ps ($rETR_{max}$) and E_k had a positive one, specifically in the –3-0˚C range (Salleh & McMinn 2011). However, alpha typically decreases in prolonged periods of darkness, such as the arctic microalgae experience in winter, meaning that we might expect a decrease in photosynthetic electron transport efficiency (Reeves et al., 2011, Veuger & van Oevelen, 2011). Additionally, ps has been demonstrated to have a positive relationship with irradiance in benthic microalgae in many studies, therefore introducing predictor variables that likely have opposite influences on ps (McMinn et al., 2004). Therefore, most of the light curve variables displayed expected increases or decreases towards the end of the sampling season but not in the first couple months of this study.

With several of the variables, most prominently alpha and Chl *a*, we can see this peak in the middle of the sample season where this shift occurs. It is possible that this switch is due to some threshold being reached which forces a physiological change for survival. Ps, for example, could have decreased with light until a temperature was reached which allowed the rETR to be maintained due to shifting to an established survival mechanisms within the algae. The physiological limits of these microalgae can be pushed from many environmental factors, including temperature, light, and oxygen availability (McMinn & Martin, 2013). There has been growing support for the theory that the rate at which diatoms within the MPB use their lipid reserves is temperature dependent, with a decreasing rate at lower temperatures (Johnsen et al., 2020). Understanding and learning about these points at which microalgae switch metabolic rates or prioritize certain strategies over others is crucial to better understanding the functioning of the MPB. More studies are needed to better define the thresholds for physical adaptation of polar microalgae as the understanding of this would be immensely beneficial (Gómez et al., 2009)

There are so many potential influencing and driving factors in these Arctic intertidal environments, and there are many reasons why the biological variables did not show a more expected response into the seasonal shift towards winter. There were also many variables that I did not account for such wave actions, daily light cycles, or inorganic nutrients concentrations. This makes it difficult to fully understand the extent to which one variable truly influenced these light curve variables, as in nature the effects occur simultaneously.

4.5 What could be done differently

Future studies should include additional variables. Grain size, for site comparison at least, should be included and was initially discussed in this project's planning but could not be implemented. Additionally, including water analysis for inorganic nitrogen, nitrate, ammonia, and phosphorus levels could have been beneficial. Additionally, the selected sample site is exposed to many potential pollutants and run-off variation from its proximity to the airport, the island snow dumping zone, and litter washing in with the tides. This could be minimized by selecting sites further away from Tromsø, which however would cause more logistical challenges and does not represent as well the exact conditions here in Tromsø closer to an urban setting.

At every sampling event, I sampled the plots in the same order, starting with block 1 plot 1. This means that all the plots were sampled at roughly the same time in the tidal cycle, making it easy to compare numbers from the same plot from week to week but possibly creating an unintentional time variable when comparing values from different plot locations. If there was any vertical migration, for example, due to time in the tidal cycle or time since first being exposed to the open air, this could have given some type of unintentional bias to the results. By using a random approach in selecting the sequence of plot measurements, this problem could be avoided.

4.6 Outlook for future research

This study clearly demonstrated that the intertidal flats at high latitudes like Tromsøya are inhabited by active microphytobenthos (MPB) communities, that do change with season. However, this study considered only a limited number of environmental factors, mainly temperature, salinity, and day of the year, all of which had significant impacts as shown in the RDA analysis. Follow-up research focused on this area of the Arctic would clearly benefit from the inclusion of more environmental variables that are known to impact microphytobenthos activity and composition. For example, sediment type, such as muddier versus sandier areas, and sediment grain size are major influencers for taxonomical variability within intertidal MPB communities (Jesus et al., 2009). Furthermore, the sediment type can affect the depth to which the MPB communities can inhabit due to differences light attenuation, sometimes meaning that the zone for MPB can vary between just the top 1mm in muddy sediments and the top few centimeters in sandy ones (Kühl & Jørgensen 1994). The abundance of benthic microorganisms is furthermore highly dependent on the grain size distribution, oxygen availability and organic matter availability in the sediment (Fenchel 1969). Sediment texture has also been shown to influence the community structure of the MPB (Malakhov 2021). Therefore, microphytobenthic studies including a sediment analysis component would be an essential step to obtaining a more holistic overview and understanding of the microalgal communities on Tromsøya in the future.
Another aspect of the environment which was not strongly considered in the context of this master's project was the proximity of sampling locations to macroalgal communities. The sampling blocks were in zones containing macroalgae, but the exact distance from macroalgae was not ever measured or standardized. However, the presence of macroalgae can cause environmental modifications, such as shading, uneven sediment surfaces, or even through providing shelter for microalgae eating fauna such as snails, significant enough to affect both spatial and temporal patchiness within the MPB (Umanzor et al., 2017, Wulff et al., 2009).

Studies focusing on Arctic benthic diatom taxa and their temperature requirements are still very much needed (Gómez et al., 2009). Despite the incredible capabilities and contributions from intertidal MPB across a broad polar distribution, primary production estimates have been underestimated for a long time due to most studies focusing on other regions of the world (Cahoon 1999). The benthic primary production contributions in the Arctic are still under sampled and poorly understood (Attard et al., 2024). Most studies on microbenthic primary productivity have been performed in temperate ecosystems, thus encouraging us in the scientific community to expand the scope of this research to arctic ecosystems as well (Gómez et al., 2009). Through my own research for this project, I've found that many studies seem to focus on MPB reactivity to increases in light and temperature as the season changes to summer and late summer rather than the transition period into winter. It would be beneficial to obtain more insight into the microphytobenthic community seasonal changes entering winter.

5 Conclusion

Following this investigation into the seasonality of the microphytobenthos (MPB) on Tromsøya from late August to mid-December, we have data to suggest an aspect of seasonality within MPB abundancy, taxa composition within the community, and activity. The results suggest that microalgal cells adjust their photosynthetic mechanisms to adapt to changes in climate conditions such as amount of daylight and temperature. Aligning with other arctic studies, this study reports high diatom make-up from surface sediment samples examined through microscopy. However, more information is needed to gain more insight and confidence into what the true drivers of MPB growth and photosynthetic activity are.

As mentioned previously, similar studies are still needed in the Arctic. The Arctic is an under-sampled region, especially in coastal areas, and further studies focusing on the functioning and seasonality of the MPB should be supported (Glud et al., 2009). The quantitative contributions of benthic primary production within Arctic coastal areas are still relatively unknown, and, especially with rapidly changing arctic conditions, learning more about the quantitative importance of the MPB will only help us to understand the functioning of Arctic ecosystems (Attard et al., 2024).

Works cited

Admiraal, W., & Peletier, H. (1979). Influence of organic compounds and light limitation on the growth rate of estuarine benthic diatoms. British Phycological Journal, 14(3), 197-206.

Attard, K., Singh, R. K., Gattuso, J. P., Filbee-Dexter, K., Krause-Jensen, D., Kühl, M., & Ardyna, M. (2024). Seafloor primary production in a changing Arctic Ocean. Proceedings of the National Academy of Sciences, 121(11), e2303366121.

Azovsky, A., Saburova, M., Tikhonenkov, D., Khazanova, K., Esaulov, A., & Mazei, Y. (2013). Composition, diversity and distribution of microbenthos across the intertidal zones of Ryazhkov Island (the White Sea). European journal of protistology, 49(4), 500-515.

Bates, D., Maechler, M., Bolker, B., Walker, S. (2015). Fitting Linear Mixed-Effects Models Using lme4. Journal of Statistical Software, 67(1), 1-48. doi:10.18637/jss.v067.i01.

Blanchard, G. F., Guarini, J. M., Orvain, F., & Sauriau, P. G. (2001). Dynamic behaviour of benthic microalgal biomass in intertidal mudflats. Journal of Experimental Marine Biology and Ecology, 264(1), 85-100.

Bos, J., & Keyzers, M. (2023). Standard Operating Procedure EA026, Version 6.0: Standard Operating Procedure EAP026, version 6.0 Chlorophyll a Analysis. 23-03-231. Washington State Department of Ecology, Olympia. https://apps.ecology.wa.gov/publications/SummaryPages/2303231.html

Böttcher, M.E., Hespenheide, B., Llobet-Brossa, E., Beardsley, C., Larsen, O., Schramm, A., Wieland, A., Böttcher, G., Berninger, U.-G., Amann, R., 2000. The biogeochemistry, stable isotope geochemistry, and microbial community structure of a temperate intertidal mudflat: an integrated study. Cont. Shelf Res. 20[12-13], 1749-1769.

Cahoon, L. B., Nearhoof, J. E., & Tilton, C. L. (1999). Sediment grain size effect on benthic microalgal biomass in shallow aquatic ecosystems. Estuaries, 22, 735-741.

Cartaxana, P., Vieira, S., Ribeiro, L., Rocha, R. J., Cruz, S., Calado, R., & da Silva, J. M. (2015). Effects of elevated temperature and CO 2 on intertidal microphytobenthos. BMC ecology, 15, 1-10.

Cartaxana, P., Cruz, S., Gameiro, C., & Kühl, M. (2016). Regulation of intertidal microphytobenthos photosynthesis over a diel emersion period is strongly affected by diatom migration patterns. Frontiers in microbiology, 7, 173173.

Cibic, T., Blasutto, O., Hancke, K., & Johnsen, G. (2007). Microphytobenthic species composition, pigment concentration, and primary production in sublittoral sediments of the Trondheimsfjord (Norway) 1. Journal of Phycology, 43(6), 1126-1137.

Cohn, S. A., Dunbar, S., Ragland, R., Schulze, J., Suchar, A., Weiss, J., & Wolske, A. (2016). Analysis of light quality and assemblage composition on diatom motility and accumulation rate. Diatom Research, 31(3), 173-184.

Consalvey, M., Perkins, R. G., Paterson, D. M., & Underwood, G. J. (2005). PAM fluorescence: a beginners guide for benthic diatomists. Diatom Research, 20(1), 1-22.

Cooksey, K. E., & Chansang, H. (1976). Isolation and physiological studies on three isolates of Amphora (Bacillariophyceae) 1. *Journal of Phycology*, *12*(4), 455-460.

Eilers, P.H.C. and Peeters, J.C.H. 1988 A model for the relationship between light intensity and the rate of photosynthesis in phytoplankton. *Ecological Modeling*. **42**, 199–215.

Fenchel, T., 1969. The ecology of marine Microbenthos IV. Structure and function of the benthic ecosystem, its chemical and physical factors and the microfauna communities with special reference to the ciliated Protozoa. Ophelia 6, 1-182.

Flaten, T. P. (1991). A nation-wide survey of the chemical composition of drinking water in Norway. Science of the total environment, 102, 35-73.

Forget, M. H., Sathyendranath, S., Platt, T., Pommier, J., Vis, C., Kyewalyanga, M. S., & Hudon, C. (2007). Extraction of photosynthesis-irradiance parameters from phytoplankton production data: demonstration in various aquatic systems. *Journal of plankton research*, *29*(3), 249-262.

Forster, G. F. B. R. M., Créach, V., Kromkamp, M., Glud, F., Maddi, S., Fry, C., ... & Brockmann, M. (2003, August). Functioning of microphytobenthos in estuaries. In Proceedings of the Colloquium (Vol. 21).

Fox J, Weisberg S (2019). _An R Companion to Applied Regression_, Third edition. Sage, Thousand Oaks CA. <https://socialsciences.mcmaster.ca/jfox/Books/Companion/>.

Gattuso, J. P., Gentili, B., Antoine, D., & Doxaran, D. (2020). Global distribution of photosynthetically available radiation on the seafloor. Earth System Science Data, 12(3), 1697-1709.

Glud, R. N., Woelfel, J., Karsten, U., Kühl, M., & Rysgaard, S. (2009). Benthic microalgal production in the Arctic: applied methods and status of the current database.

Goessling, J. W., Su, Y., Cartaxana, P., Maibohm, C., Rickelt, L. F., Trampe, E. C., ... & Kühl, M. (2018). Structure-based optics of centric diatom frustules: modulation of the in vivo light field for efficient diatom photosynthesis. New Phytologist, 219(1), 122-134.

Gómez, I., Wulff, A., Roleda, M. Y., Huovinen, P., Karsten, U., Quartino, M. L., ... & Wiencke, C. (2009). Light and temperature demands of marine benthic microalgae and seaweeds in polar regions.

Guarini, J. M., Blanchard, G. F., & Richard, P. (2006). Modelling the dynamics of the microphytobenthic biomass and primary production in European intertidal mudflats. Functioning of microphytobenthos in estuaries, 187-226.

Hall, C. M., Brekke, A., & Cannon, P. S. (2007, November). Climatic trends in E-region critical frequency and virtual height above Tromsø (70° N, 10° E). In Annales

Geophysicae (Vol. 25, No. 11, pp. 2351-2357). Göttingen, Germany: Copernicus Publications.

Höper, J., Jegstad, K. M., & Remmen, K. B. (2022). Student teachers' problem-based investigations of chemical phenomena in the nearby outdoor environment. Chemistry Education Research and Practice, 23(2), 361-372.

Jakobsson, M., Mayer, L. A., Bringensparr, C., Castro, C. F., Mohammad, R., Johnson, P., ... & Zinglersen, K. B. (2020). The international bathymetric chart of the Arctic Ocean version 4.0. Scientific data, 7(1), 176.

Jesus, B., Brotas, V., Ribeiro, L., Mendes, C. R., Cartaxana, P., & Paterson, D. M. (2009). Adaptations of microphytobenthos assemblages to sediment type and tidal position. Continental Shelf Research, 29(13), 1624-1634.

Jesus, B., Jauffrais, T., Trampe, E., Méléder, V., Ribeiro, L., Bernhard, J. M., ... & Kühl, M. (2023). Microscale imaging sheds light on species-specific strategies for photo-regulation and photo-acclimation of microphytobenthic diatoms. Environmental Microbiology, 25(12), 3087-3103.

Johnsen, G., Leu, E., & Gradinger, R. (2020). Marine micro-and macroalgae in the polar night. Polar night marine ecology: life and light in the dead of night, 67-112.

Karsten, U., Schaub, I., Woelfel, J., Sevilgen, D. S., Schlie, C., Becker, B., ... & Wagner, H. (2019). Living on cold substrata: new insights and approaches in the study of microphytobenthos ecophysiology and ecology in Kongsfjorden. The Ecosystem of Kongsfjorden, Svalbard, 303-330.

Kühl, M. J0rgensen BB (1994) The light field of microbenthic communities: radiance distribution and microscale optics of sandy coastal sediments. *Limnol Oceanogr39*, 1368-1398.

Langtidsvarsel for tromsø: Værvarsel. Yr. (2023). https://www.yr.no/nb/v%C3%A6rvarsel/daglig-tabell/1-305409/Norge/Troms/Troms%C3%B8/Troms%C3%B8

Launeau, P., Méléder, V., Verpoorter, C., Barillé, L., Kazemipour-Ricci, F., Giraud, M., Le Menn, E. (2018). Microphytobenthos biomass and diversity mapping at different spatial scales with a hyperspectral optical model. Remote Sensing, 10(5), 716.

Leu, E., Wängberg, S. Å., Wulff, A., Falk-Petersen, S., Ørbæk, J. B., & Hessen, D. O. (2006). Effects of changes in ambient PAR and UV radiation on the nutritional quality of an Arctic diatom (Thalassiosira antarctica var. borealis). Journal of Experimental Marine Biology and Ecology, 337(1), 65-81.

MacIntyre, H. L., Geider, R. J., & Miller, D. C. (1996). Microphytobenthos: the ecological role of the "secret garden" of unvegetated, shallow-water marine habitats. I. Distribution, abundance and primary production. Estuaries, 19, 186-201.

Malakhov, Y. (2021). Sediment nutrients and mud content as driving factors of intertidal microphytobenthos in the estuaries of South Island, New Zealand.

McGee, D., Laws, R. A., & Cahoon, L. B. (2008). Live benthic diatoms from the upper continental slope: extending the limits of marine primary production. Marine Ecology Progress Series, 356, 103-112.

McMinn, A., Runcie, J. W., & Riddle, M. (2004). EFFECT OF SEASONAL SEA ICE BREAKOUT ON THE PHOTOSYNTHESIS OF BENTHIC DIATOM MATS AT CASEY, ANTARCTICA 1. Journal of phycology, 40(1), 62-69.

McMinn, A., & Hegseth, E. N. (2004). Quantum yield and photosynthetic parameters of marine microalgae from the southern Arctic Ocean, Svalbard. Journal of the Marine Biological Association of the United Kingdom, 84(5), 865–871.

McMinn, A., & Martin, A. (2013). Dark survival in a warming world. Proceedings of the Royal Society B: Biological Sciences, 280(1755), 20122909.

Oakes, J. M., Rysgaard, S., Glud, R. N., & Eyre, B. D. (2016). The transformation and fate of sub-Arctic microphytobenthos carbon revealed through 13C-labeling. Limnology and Oceanography, 61(6), 2296-2308.

Observasjoner og værstatistikk. Norsk Klima Service Senter. (2023). https://seklima.met.no/observations/

Oksanen J, Simpson G, Blanchet F, Kindt R, Legendre P, Minchin P, O'Hara R, Solymos P, Stevens M, Szoecs E, Wagner H, Barbour M, Bedward M, Bolker B, Borcard D, Carvalho G, Chirico M, De Caceres M, Durand S, Evangelista H, FitzJohn R, Friendly M, Furneaux B, Hannigan G, Hill M, Lahti L, McGlinn D, Ouellette M, Ribeiro Cunha E, Smith T, Stier A, Ter Braak C, Weedon J (2022). _vegan: Community Ecology Package_. R package version 2.6-4, <https://CRAN.R-project.org/package=vegan>.

Perkins, R. G., K. Oxborough, A. R. M. Hanlon, G. J. C. Underwood, and N. R. Baker. (2002). Can chlorophyll fluorescence be used to estimate the rate of photosynthetic electron transport within microphytobenthic biofilms? Mar. Ecol. Prog. Ser. 228: 47-56.

Pessarrodona, A., Assis, J., Filbee-Dexter, K., Burrows, M. T., Gattuso, J. P., Duarte, C. M., ... & Wernberg, T. (2022). Global seaweed productivity. Science advances, 8(37), eabn2465.

Pinckney, J. L., & Zingmark, R. G. (1991). Effects of tidal stage and sun angles on intertidal benthic microalgal productivity. Marine ecology progress series, 76, 81.

PSI (Photon Systems Instruments). (2023). Instruction Guide AquaPen-C AP 110-C & AquaPen-P AP 110-P. https://handheld.psi.cz/documents/AquaPen_manual_2023-07.pdf

Ralph, P. J., & Gademann, R. (2005). Rapid light curves: a powerful tool to assess photosynthetic activity. Aquatic botany, 82(3), 222-237.

Reeves, S., McMinn, A., & Martin, A. (2011). The effect of prolonged darkness on the growth, recovery and survival of Antarctic sea ice diatoms. Polar biology, 34, 1019-1032.

Salleh, S., & McMinn, A. (2011). Photosynthetic response and recovery of Antarctic marine benthic microalgae exposed to elevated irradiances and temperatures. Polar Biology, 34, 855-869.

Sandrini-Neto, L. & Camargo, M.G. (2023).GAD: an R package for ANOVA designs from general principles. Available on CRAN.

Saroussi, S., & Beer, S. (2007). Alpha and quantum yield of aquatic plants derived from PAM fluorometry: uses and misuses. Aquatic Botany, 86(1), 89-92.

Scholz, B., & Liebezeit, G. (2012). Microphytobenthic dynamics in a Wadden Sea intertidal flat–Part II: Seasonal and spatial variability of non-diatom community components in relation to abiotic parameters. *European Journal of Phycology*, *47*(2), 120-137.

Scholz, B., & Einarsson, H. (2015). Microphytobenthic community composition of two sub-Arctic intertidal flats in Huna Bay (Northern Iceland). European journal of phycology, 50(2), 182-206.

Semcheski, M. R., Egerton, T. A., & Marshall, H. G. (2016). Composition and diversity of intertidal microphytobenthos and phytoplankton in Chesapeake Bay. *Wetlands*, *36*, 483-496.

Serôdio, J., & Paterson, D. M. (2022). Role of Microphytobenthos in the Functioning of Estuarine and Coastal Ecosystems. In Life Below Water (pp. 894-906). Cham: Springer International Publishing.

Sevilgen, D. S., de Beer, D., Al-Handal, A. Y., Brey, T., & Polerecky, L. (2014). Oxygen budgets in subtidal arctic (Kongsfjorden, Svalbard) and temperate (Helgoland, North Sea) microphytobenthic communities. Marine Ecology Progress Series, 504, 27-42.

Silsbe GM, Malkin SY (2015). _phytotools: Phytoplankton Production Tools_. R package version 1.0, <https://CRAN.R-project.org/package=phytotools>.

Snoeijs, P. J. (1990). Effects of temperature on spring bloom dynamics of epilithic diatom communities in the Gulf of Bothnia. Journal of Vegetation Science, 1(5), 599-608.

Solar Calculation Details: NOAA_Solar_Calculations_Day.xls. National Oceanic & Atmospheric Administration (NOAA) Global Monitoring Laboratory. (n.d.). https://gml.noaa.gov/grad/solcalc/calcdetails.html

Stumm, K., & Berninger, U. G. (2005). Seasonal changes of a benthic microbial community in an intertidal fine sediment. Untersuchung zur Diversität und Funktion benthischer Mikroalgen und Protozoen im Nahrungsnetz mariner und limnischer Sedimente, 25.

Sundbäck, K., & Jönsson, B. (1988). Microphytobenthic productivity and biomass in sublittoral sediments of a stratified bay, southeastern Kattegat. Journal of Experimental Marine Biology and Ecology, 122(1), 63-81.

Sundbäck, K., Linares, F., Larson, F., Wulff, A., & Engelsen, A. (2004). Benthic nitrogen fluxes along a depth gradient in a microtidal fjord: the role of denitrification and microphytobenthos. Limnology and Oceanography, 49(4), 1095-1107.

Taasen, J. P., & Høisæter, T. (1981). The shallow-water soft-bottom benthos in lindåspollene, western Norway: 4. Benthig marine diatoms, seasonal density fluctuations. Sarsia, 66(4), 293-316.

Umanzor, S., Ladah, L., & Zertuche-González, J. A. (2017). The influence of species, density, and diversity of macroalgal aggregations on microphytobenthic settlement. Journal of phycology, 53(5), 1060-1071.

Vannstand og tidevann: Resultat for Tromsø lufthavn, Langnes (Tromsø). Kartverket.no. (2023). https://www.kartverket.no/til-sjos/se-havniva/resultat?id=691534&location=Troms%C3%B8+lufthavn%2C+Langnes

Veuger, B., & van Oevelen, D. (2011). Long-term pigment dynamics and diatom survival in dark sediment. Limnology and Oceanography, 56(3), 1065-1074.

Wickham, H. (2016) ggplot2: Elegant Graphics for Data Analysis. Springer-Verlag New York.

Wickham H, Averick M, Bryan J, Chang W, McGowan LD, François R, Grolemun G, Haye A, Henr L, Heste J, Kuh M, Pederse TL, Mille E, Bach SM, Müll K, Oo ,J, Robins ,D, Seid ,DP, Spi,V, Takahas ,K, Vaugh ,D, Wil ,C, W ,K, Yutani ,H (2019). "Welcome to the tidyverse."_Journal of Open Source Software_, *4*(43), 1686. doi:10.21105/joss.01686 <https://doi.org/10.21105/joss.01686>.

Wickham H, Francois R, Henry L, Muller K, Vaughan D (2023). _dplyr: A Grammar of Data Manipulation_. R package version 1.1.4, <https://CRAN.R-project.org/package=dplyr>.

Wickham H, Vaughan D, Girlich M (2024). _tidyr: Tidy Messy Data_. R package version 1.3.1, <https://CRAN.R-project.org/package=tidyr>.

Wright K (2021). _corrgram: Plot a Correlogram_. R package version 1.14, <https://CRAN.R-project.org/package=corrgram>.

Woelfel, J., Schumann, R., Leopold, P., Wiencke, C. & Karsten, U.(2009). Microphytobenthic biomass along gradients of physicalconditions in Arctic Kongsfjorden, Svalbard.Botanica Marina,52: 573–583.

Woelfel, J., Schumann, R., Peine, F., Flohr, A., Kruss, A., Tegowski, J., ... & Karsten, U. (2010). Microphytobenthos of Arctic Kongsfjorden (Svalbard, Norway): biomass and potential primary production along the shore line. Polar Biology, 33, 1239-1253.

Woelfel, J., Eggert, A., & Karsten, U. (2014). Marginal impacts of rising temperature on Arctic benthic microalgae production based on in situ measurements and modelled estimates. Marine Ecology Progress Series, 501, 25-40.

Wulff, A., Iken, K., Quartino, M. L., Al-Handal, A., Wiencke, C., & Clayton, M. N. (2009). Biodiversity, biogeography and zonation of marine benthic micro-and macroalgae in the Arctic and Antarctic.

Varela, M., & Penas, E. (1985). Primary production of benthic microalgae in an intertidal sand flat of the Ria de Arosa, NW Spain. *Marine Ecology Progress Series*, *25*(2), 111-119.

Appendix

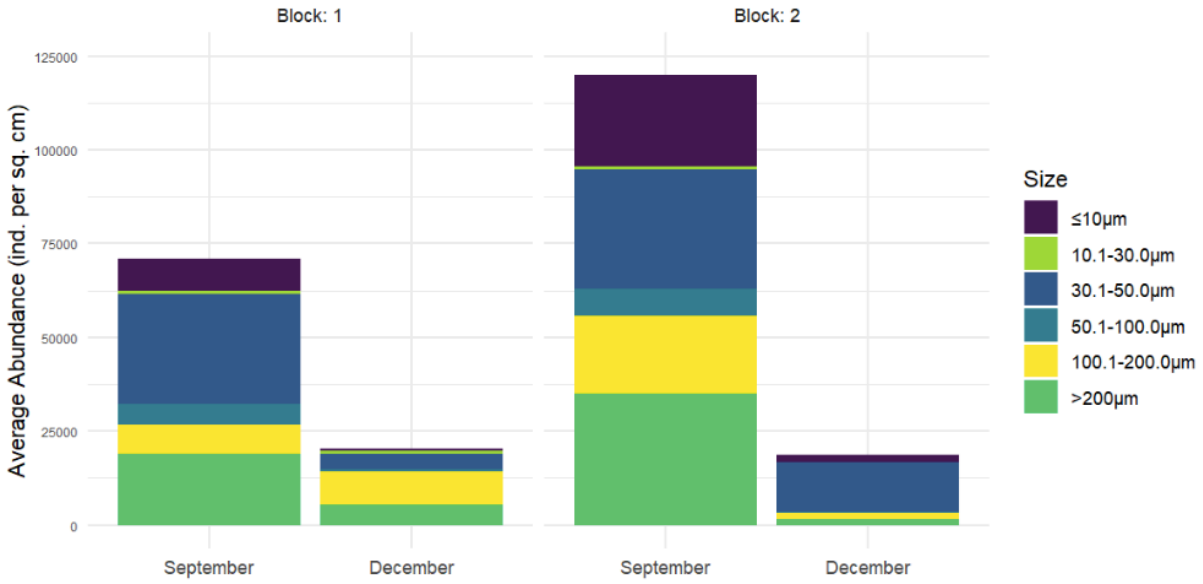

***Figure 1 (Appendix)**: Rough size break down of algae looked at through microscopy work.*

Dependent (response) variable		Significant source of variance	SS	df	MS	F	p-value
Chl *a*	(µg/cm^{-2})	Block	8.79E+01	5	17.59	1.11	0.36
		Day of year	67.2	1	67.23	4.02	0.049
		Block x Day of year	1.27E+02	5	25.4	1.604	0.17
		Residuals	1070.3	64	16.72		
alpha	(µmol photons m^{-2}s^{-1})	Block	0.032	1	0.03202	16.234	7.32E-05
		Day of year	0.8792	16	0.05495	27.856	<2e-16
		Block x Day of year	0.0664	16	0.00415	2.103	0.0086
		Residuals	0.5227	265	0.00197		
ps	(µmol electrons m^{-2}s^{-1})	Block	9.49E+03	1	9492	2.434	0.11
		Day of year	166007	16	10375	2.647	0.00067
		Block x Day of year	8.53E+04	16	5333	1.398	0.14
		Residuals	1010686	265	3814		
Qmax		Block	5.90E-03	1	0.0059	0.73	0.39
		Day of year	2.915	16	0.18219	21.61	<2e-16
		Block x Day of year	2.51E-01	16	0.01567	1.958	0.161
		Residuals	2.385	283	0.00843		
Ek	(µmol photons m^{-2}s^{-1})	Block	3.61E+04	1	36074	0.446	0.505
		Day of year	7922170	16	495136	6.094	1.50E-11
		Block x Day of year	1.43E+06	16	89642	1.108	3.47E-01
		Residuals	22910628	282	81243		
F_o	(RFU)	Block	9.56E+04	1	95599	0.001	0.97
		Day of year	8.58E+09	16	535978619	6.077	2.08E-11
		Block x Day of year	2.74E+09	16	171205436	1.941	0.0173
		Residuals	2.35E+10	266	88202741		

***Figure 2 (Appendix)**: Full results (including insignificant ones) from the ANOVA tests run with block x day of the year on the response variables.*

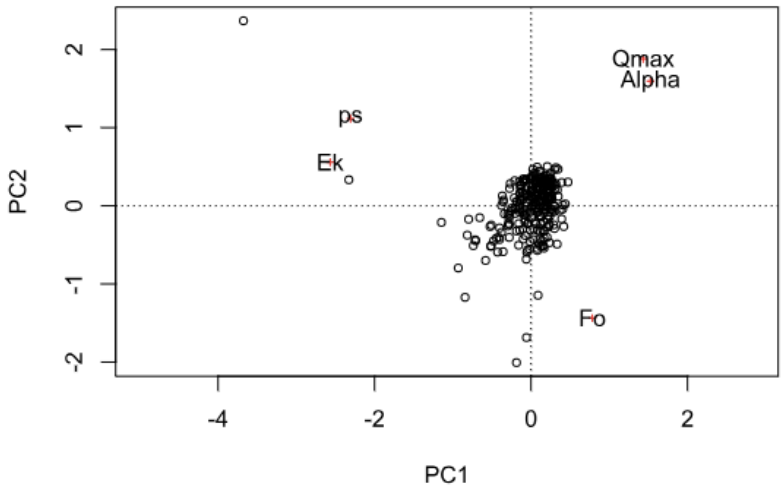

***Figure 3 (Appendix)**: Basic principal analysis (PCA) plot with the biological response variables obtained through all LC3 measurements made with the AquaPen throughout the entire sample season.*

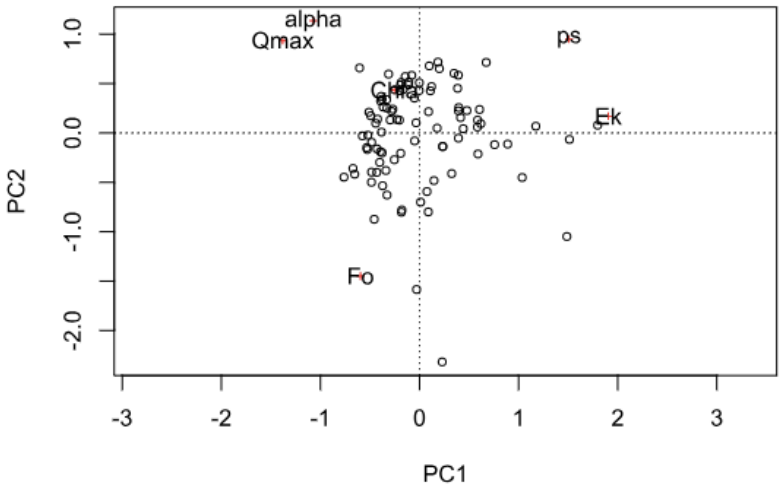

***Figure 4 (Appendix)**: Basic principal analysis (PCA) plot for data subset including chlorophyll a concentration data. Only one LC3 measurement per plot per day is included in this subset since only one sediment sample per plot was taken each sample day for chlorophyll a analysis.*

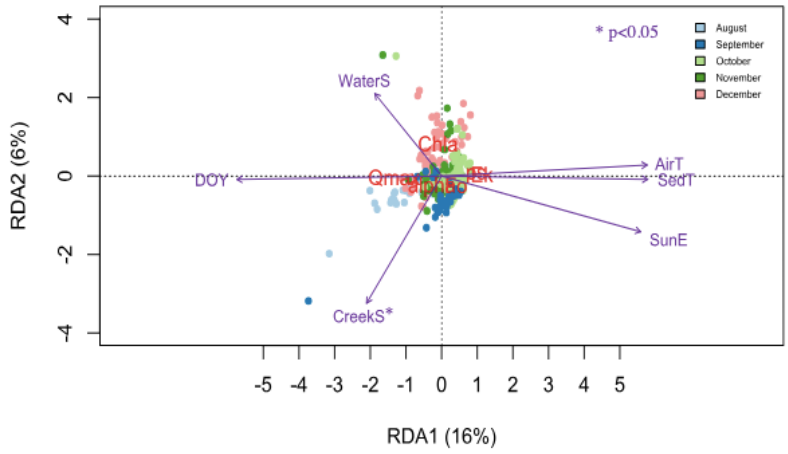

***Figure 5 (Appendix)**: Redundancy analysis performed on a subset of the data to include chlrophyll a.*

Data from Chl *a* lab work:

Sample Date	PlotID	Chl (µg/L)	Chl(ug/cm^2)
31-Aug-2023	B1P1	66.81495945	9.450489333
31-Aug-2023	B1P2	77.07553051	10.90177237
31-Aug-2023	B1P3	52.6948293	7.453299776
31-Aug-2023	B2P1	45.69968125	6.463887037
31-Aug-2023	B2P2	60.31473101	8.531079368
31-Aug-2023	B2P3	36.95526173	5.22705259
7-Sep-2023	B1P1	44.49455006	6.293430008
7-Sep-2023	B1P2	70.72935888	10.00415262
7-Sep-2023	B1P3	24.63788693	3.484849644
7-Sep-2023	B2P1	41.75543937	5.906002753
7-Sep-2023	B2P2	45.18344561	6.390869265
7-Sep-2023	B2P3	15.02222287	2.124784003
15-Sep-2023	B1P1	47.34993004	6.697302708
15-Sep-2023	B1P2	36.52060837	5.165574038
15-Sep-2023	B1P3	24.00480065	3.395304201
15-Sep-2023	B2P1	29.20455708	4.130771873
15-Sep-2023	B2P2	-0.13851742	-0.01959228
15-Sep-2023	B2P3	19.00134554	2.68760192
20-Sep-2023	B1P1	62.43819581	8.831427997
20-Sep-2023	B1P2	62.35157518	8.819176141
20-Sep-2023	B1P3	49.11896729	6.947520141
20-Sep-2023	B2P1	50.26790166	7.110028538
20-Sep-2023	B2P2	16.07445994	2.273615273
20-Sep-2023	B2P3	19.09106667	2.700292321
29-Sep-2023	B1P1	32.27270986	4.564739736
29-Sep-2023	B1P2	27.09620729	3.832561152
29-Sep-2023	B1P3	0.362603221	0.051287584
29-Sep-2023	B2P1	17.46504065	2.470302785
29-Sep-2023	B2P2	36.14777152	5.11283898
29-Sep-2023	B2P3	22.16135106	3.134561684
3-Oct-2023	B1P1	-46.1288351	-6.524587719
3-Oct-2023	B1P2	62.28685195	8.81002151
3-Oct-2023	B1P3	23.85616974	3.374281441
3-Oct-2023	B2P1	71.2436567	10.0768963
3-Oct-2023	B2P2	95.76872561	13.54578866
3-Oct-2023	B2P3	0.981737191	0.138859575
13-Oct-2023	B1P1	90.16803391	12.75361161
13-Oct-2023	B1P2	54.93572609	7.770258303
13-Oct-2023	B1P3	58.43601306	8.2653484
13-Oct-2023	B2P1	43.10706987	6.097181041
13-Oct-2023	B2P2	42.98750628	6.080269643
13-Oct-2023	B2P3	75.63146592	10.69751996
16-Oct-2023	B1P1	56.87471028	8.044513494
16-Oct-2023	B1P2	92.24363452	13.0471902
16-Oct-2023	B1P3	127.4470688	18.02645956
16-Oct-2023	B2P1	68.62798524	9.706928626
16-Oct-2023	B2P2	44.78154143	6.334022846
16-Oct-2023	B2P3	82.79849874	11.71124454
27-Oct-2023	B1P1	67.3680137	9.52871483
27-Oct-2023	B1P2	88.03081057	12.45131694
27-Oct-2023	B1P3	127.1116319	17.97901445
27-Oct-2023	B2P1	81.10271115	11.47138774
27-Oct-2023	B2P2	40.08406833	5.669599493
27-Oct-2023	B2P3	88.18079796	12.47253156
1-Nov-2023	B1P1	53.40058389	7.553123622
1-Nov-2023	B1P2	45.33692107	6.412577251
1-Nov-2023	B1P3	114.6607412	16.21792665
1-Nov-2023	B2P1	45.7979288	6.477783437
1-Nov-2023	B2P2	86.57666932	12.24563925
1-Nov-2023	B2P3	77.9223585	11.02155002
6-Nov-2023	B1P1	58.19339781	8.23103224
6-Nov-2023	B1P2	76.72672264	10.85243604
6-Nov-2023	B1P3	103.6591472	14.66183132
6-Nov-2023	B2P1	112.5963799	15.92593779
6-Nov-2023	B2P2	58.27032932	8.241913642
6-Nov-2023	B2P3	51.41373551	7.27209839
10-Nov-2023	B1P1	63.90551425	9.038969502
10-Nov-2023	B1P2	67.02637577	9.480392633
10-Nov-2023	B1P3	84.5305236	11.95622684

10-Nov-2023 B2P1	112.9684417	15.97856321
10-Nov-2023 B2P2	99.96837236	14.1397981
10-Nov-2023 B2P3	89.83414726	12.70638578
15-Nov-2023 B1P1	38.87292989	5.498292783
15-Nov-2023 B1P2	64.37349814	9.105162415
15-Nov-2023 B1P3	86.98438696	12.30330794
15-Nov-2023 B2P1	62.33820422	8.817284915
15-Nov-2023 B2P2	76.08375346	10.76149273
15-Nov-2023 B2P3	34.20781841	4.838446745
21-Nov-2023 B1P1	55.95463263	7.914375212
21-Nov-2023 B1P2	57.64693215	8.153738652
21-Nov-2023 B1P3	126.109003	17.8371999
21-Nov-2023 B2P1	7.270743087	1.02839365
21-Nov-2023 B2P2	5.547825991	0.784699576
21-Nov-2023 B2P3	46.40388559	6.56349161
30-Nov-2023 B1P1	28.03411289	3.965221068
30-Nov-2023 B1P2	30.3290749	4.289826727
30-Nov-2023 B1P3	48.50932865	6.861291195
30-Nov-2023 B2P1	7.620132303	1.077812209
30-Nov-2023 B2P2	30.5472736	4.320689344
30-Nov-2023 B2P3	12.56797194	1.777648086
7-Dec-2023 B1P1	15.3063075	2.164965705
7-Dec-2023 B1P2	24.82585562	3.511436446
7-Dec-2023 B1P3	21.2912692	3.011494943
7-Dec-2023 B2P1	60.82961018	8.603905277
7-Dec-2023 B2P2	31.86014766	4.506385818
7-Dec-2023 B2P3	27.85970896	3.940552902
14-Dec-2023 B1P1	35.62300945	5.038615209
14-Dec-2023 B1P2	42.76291277	6.048502526
14-Dec-2023 B1P3	35.24416535	4.98503047
14-Dec-2023 B2P1	41.40837554	5.856913102
14-Dec-2023 B2P2	35.13080279	4.968996162
14-Dec-2023 B2P3	27.35490646	3.869152265

Date	Blank Rb RFU value	Blank Ra RFU value
14-Mar-2024	769.68	806.4
15-Mar-2024	722.37	788.2
16-Mar-2024	793.34	1017.21
19-Mar-2024	788.4	865.02
19-Mar-2024	960.52	813.43

Raw Data

Environmental data collected during field work and master data sheet including light curve parameter estimates calculated with phytotools package in Rstudio.

Date:	Block	Block salinity (sal ppt)	Block water T (˚C)	ocean salinity (sal ppt)	Ocean T (˚C)
31-Aug-2023	1	20.8	14	34.6	11.8
31-Aug-2023	2	1.9	13.2	31.2	12.3
7-Sep-2023	1	28	14.4	34.1	12.5
7-Sep-2023	2	2.2	12.1	18.2	12.1
15-Sep-2023	1	14.8	7.6	33.9	7.9
15-Sep-2023	2	8.4	8.3	33.6	8.8
20-Sep-2023	1	18.8	7.8	32.6	7.4
20-Sep-2023	2	0.7	8.2	34.5	8.2
29-Sep-2023	1	19.1	8.4	33.7	8.6
29-Sep-2023	2	14.3	8.7	33.4	8.9
3-Oct-2023	1	9.9	8	33.7	8
3-Oct-2023	2	4	7.1	34.4	7.5
13-Oct-2023	1	25.7	4.3	30.7	5.1
13-Oct-2023	2	9.6	4	21.2	4.9
16-Oct-2023	1	25.6	5.6	31.4	5.8
16-Oct-2023	2	11.7	5.5	34.4	6.1
27-Oct-2023	1	23.1	3.8	33.4	3.9
27-Oct-2023	2	15.7	3.4	34.8	4.5
1-Nov-2023	1	19.6	3	35.3	4
1-Nov-2023	2	5.5	2.3	34.7	4.1
6-Nov-2023	1	28.5	2.6	34.1	3.6
6-Nov-2023	2	8.4	3.1	27.2	3.6
10-Nov-2023	1	15.4	1.9	34.4	3.5
10-Nov-2023	2	11.8	1.6	30	3
15-Nov-23	1	NA	NA	NA	NA
15-Nov-23	2	NA	NA	NA	NA
21-Nov-23	1	33.8	-1.9	34.2	-1.5
21-Nov-23	2	1.5	-0.2	31.6	1.6
30-Nov-23	1	17.5	-0.4	35.5	0.3
30-Nov-23	2	3.9	-1.4	33.5	1.9
7-Dec-23	1	6.5	0.4	34.9	0.6
7-Dec-23	2	37.6	-2.1	35	0.9
14-Dec-23	1	28.9	-1.6	34	0.1
14-Dec-23	2	5.9	-1.2	34.4	-0.8

Date:	creek salinity (sal ppt)	creek T (˚C)	average light measurement (µmol photons m-2s-1)
31-Aug-2023	0.4	10.9	514.7
7-Sep-2023	0.3	10.5	246.93
15-Sep-2023	0.4	7.8	122.04
20-Sep-2023	0.3	7.9	203.77
29-Sep-2023	1.2	8.3	33.808
3-Oct-2023	0.7	7.6	107.44
13-Oct-2023	0.2	3.2	1.081
16-Oct-2023	0.2	4.9	20.768
27-Oct-2023	0.7	3.6	0.3524
1-Nov-2023	0.6	3.3	10.52
6-Nov-2023	0.7	2.8	10.28
10-Nov-2023	0.7	2.3	0
15-Nov-2023	NA	NA	0.2234
21-Nov-2023	0.4	0.8	4.8177
30-Nov-2023	0.5	0.3	0.04033
7-Dec-2023	0.7	0	0
14-Dec-2023	0.7	-0.1	0

ID	DOY	Time	AirT	SedT	Alpha	ps	Qmax	Ek	Fo
1B1P1R1	243	8:44	12.8	11.7	0.255277	82.25811	0.38	322.2302	1346
1B1P1R2	243	8:53	12.8	11.6	0.114095	353.8081	0.33	3100.995	454
1B1P1R3	243	8:59	12.2	11.9	0.289724	131.774	0.58	454.8256	3251
1B1P2R1	243	9:06	12.1	12	0.134087	66.21328	0.24	493.8097	773
1B1P2R2	243	9:12	12.3	12.1	0.229932	105.7985	0.5	460.13	5300
1B1P2R3	243	9:20	12.2	12.1	0.185142	161.1109	0.37	870.2033	1186
1B1P3R1	243	9:26	12.5	12.3	0.154485	133.1294	0.31	861.7601	967
1B1P3R2	243	9:33	12.3	12.6	0.157238	199.546	0.29	1269.071	862
1B1P3R3	243	9:40	12.3	12.1	0.194985	142.2133	0.41	729.3554	1456
1B2P1R1	243	9:58	11.9	12.6	0.168817	118.0436	0.28	699.2419	1555
1B2P1R2	243	10:04	12	12.8	0.153213	112.1179	0.31	731.777	878
1B2P1R3	243	10:10	13.1	12.8	0.20468	114.6078	0.4	559.9355	3382
1B2P2R1	243	10:17	12.6	12.8	0.053789	38.06999	0.05	707.7599	849
1B2P2R2	243	10:24	12.5	12.8	0.140236	105.6839	0.29	753.6123	1465
1B2P2R3	243	10:31	12.8	12.8	0.082834	80.1669	0.18	967.7999	604
1B2P3R1	243	10:38	13.1	13.2	0.212285	118.2115	0.37	556.8539	3360
1B2P3R2	243	10:44	12.3	13	0.176085	85.12098	0.35	483.4096	3576
1B2P3R3	243	10:50	12.7	12.8	0.172171	80.58495	0.3	468.0511	1426
2B1P1R1	250	12:34	13.4	13.5	0.21737	82.80659	0.36	380.948	1815
2B1P1R2	250	12:43	13.6	13.9	0.183974	77.96615	0.38	423.7885	3021
2B1P1R3	250	12:51	14.4	13.5	0.212342	88.26116	0.34	415.6548	6762
2B1P2R1	250	12:59	13.9	13.9	0.241384	63.5395	0.4	263.2295	18433
2B1P2R2	250	13:06	14.2	14.4	0.202576	93.181	0.25	459.9796	3089
2B1P2R3	250	13:14	14.7	13.8	0.310155	42.75326	0.6	137.8446	30365
2B1P3R1	250		12.2	14.1	0.206244	43.19701	0.46	209.4466	62876
2B1P3R2	250	13:31	14	13.9	0.154547	67.00307	0.42	433.5458	14499
2B1P3R3	250	13:38	14	13.7	0.30596	44.57436	0.5	145.6871	38948
2B2P1R1	250	14:18	13.5	12.3	0.300374	30.4845	0.55	101.4884	30853
2B2P1R2	250	14:25	13.6	12.2	0.245298	57.25371	0.48	233.4045	11476
2B2P1R3	250	14:33	13.4	12.3	0.325894	40.66757	0.59	124.7879	29975
2B2P2R1	250	14:40	13.4	12.3	0.274725	68.21613	0.5	248.3068	13004
2B2P2R2	250	14:48	13.4	12.2	0.294865	40.54332	0.52	137.4979	31601

2B2P2R3	250	14:55	13.4	12.3	0.278561	74.24728	0.43	266.5383	8843
2B2P3R1	250	15:03	13.4	12.3	0.214399	95.29312	0.4	444.4665	3837
2B2P3R2	250	15:11	13.2	12.2	0.164405	59.77564	0.3	363.5886	1954
2B2P3R3	250	15:18	13	12.3	0.287495	62.8537	0.48	218.6255	14045
3B1P1R1	258	7:19	5.5	5.6	0.223802	88.05357	0.53	393.4434	3609
3B1P1R2	258	7:28	4.9	5.5	0.210188	112.0407	0.57	533.0513	3349
3B1P1R3	258	7:35	4.2	5.8	0.209363	98.26317	0.61	469.3434	28968
3B1P2R1	258	7:44	5.4	5.5	0.169041	65.93498	0.53	390.0522	3609
3B1P2R2	258	7:52	4.8	5.5	0.351946	49.27371	0.49	140.0035	2931
3B1P2R3	258	7:59	4.7	5.6	0.327423	61.27727	0.53	187.1503	7836
3B1P3R1	258	8:07	5	5.8	0.315795	26.26168	0.52	83.1604	9981
3B1P3R2	258	8:15	5.9	5.6	0.257247	29.78489	0.57	115.7833	20482
3B1P3R3	258	8:22	5.4	5.7	0.213088	36.49173	0.53	171.2521	19506
3B2P1R1	258	9:04	7.8	7.8	0.41401	28.53868	0.00	68.93228	11606
3B2P1R2	258	9:13	6.8	8	0.222316	39.19815	0.58	176.3174	33128
3B2P1R3	258	9:20	7.3	8.1	0.259954	43.58324	0.50	167.6578	7510
3B2P2R1	258	9:28	7.1	7.8	0.228018	42.52178	0.48	186.4844	24546
3B2P2R2	258	9:35	7.1	8	0.20809	32.72151	0.45	157.2473	19539
3B2P2R3	258	9:44	7.2	8.3	0.533235	27.25132	0.55	51.10567	17263
3B2P3R1	258	9:51	6.1	8.6	0.26358	38.28817	0.56	145.2623	34787
3B2P3R2	258	9:59	6.8	8.3	0.256772	38.33755	0.55	149.3056	33356
3B2P3R3	258	10:06	7.1	8.5	0.30714	24.94182	0.53	81.20678	33941
4B1P1R1	263	9:42	7.5	6.7	0.318216	90.43116	0.38	284.1814	3061
4B1P1R2	263	9:55	7.7	6.4	0.349227	94.38356	0.35	270.2641	1326
4B1P1R3	263	10:04	7.5	6.6	0.31944	22.64204	0.32	70.88039	1306
4B1P2R1	263	10:12	6.3	6.9	0.319185	90.35769	0.27	283.0889	1824
4B1P2R2	263	10:19	7.5	7.2	0.314762	90.73459	0.45	288.2637	9201
4B1P2R3	263	10:27	7.5	7.2	0.327493	66.88013	0.40	204.2185	3901
4B1P3R1	263	10:36	7.6	7.2	0.287533	63.19091	0.50	219.7691	41322
4B1P3R2	263	10:43	7.4	7.2	0.303795	38.13469	0.47	125.5276	25944
4B1P3R3	263	10:52	7.6	7.2	0.298778	37.78146	0.49	126.4534	10728
4B2P1R1	263	11:28	8.3	8.5	NA	NA	0.50	#VALUE!	31373
4B2P1R2	263	11:36	8	7.9	0.314061	34.61886	0.45	110.2297	16483

4B2P1R3	263	11:43	8.1	8.2	0.289024	84.48943	0.42	292.327	17654
4B2P2R1	263	11:51	8.4	8.4	0.261537	38.27029	0.36	146.3287	7185
4B2P2R2	263	11:58	8.2	8.3	0.235953	41.32692	0.46	175.1488	10762
4B2P2R3	263	12:06	8.4	8.4	0.293523	34.33881	0.55	116.9884	23278
4B2P3R1	263	12:13	8	8.4	0.29519	42.92656	0.52	145.4203	37095
4B2P3R2	263	12:22	8.3	8.5	0.29494	38.2185	0.46	129.5808	27764
4B2P3R3	263	12:30	8.4	8.5	0.29199	39.62335	0.58	135.7009	28057
5B1P1R1	272	7:12	7.8	7.9	0.353574	106.0349	0.60	299.8944	2273
5B1P1R2	272	7:19	7.8	7.9	0.362552	111.0351	0.55	306.2602	1585
5B1P1R3	272	7:27	8	7.9	0.349457	30.74538	0.66	87.98056	21295
5B1P2R1	272	7:34	7.8	7.9	0.453635	47.99067	0.67	105.7915	20157
5B1P2R2	272	7:42	8	7.9	0.36013	40.4565	0.66	112.3385	15377
5B1P2R3	272	7:49	8.3	7.9	0.417652	110.4429	0.59	264.4375	3021
5B1P3R1	272	7:57	8	8	0.383827	85.44621	0.60	222.6166	4486
5B1P3R2	272	8:04	8.3	8.1	0.400772	37.04483	0.66	92.43364	33616
5B1P3R3	272	8:16	8.3	8.1	0.357551	68.67469	0.63	192.0698	8875
5B2P1R1	272	8:34	8.5	8.4	0.328836	89.00501	0.47	270.6669	1794
5B2P1R2	272	8:41	8.4	8.5	0.366327	59.79985	0.65	163.2419	18596
5B2P1R3	272	8:49	8.3	8.6	0.373375	121.8892	0.56	326.4529	3934
5B2P2R1	272	8:56	8.7	8.6	0.397737	32.92864	0.65	82.78994	19539
5B2P2R2	272	9:04	9	8.8	0.45916	68.30216	0.60	148.7547	16515
5B2P2R3	272	9:11	8.5	9	0.353337	34.8515	0.64	98.63538	25619
5B2P3R1	272	9:19	9.1	8.9	0.455557	52.98453	0.64	116.3072	38330
5B2P3R2	272	9:26	9.4	8.9	0.360154	74.02832	0.64	205.5466	17621
5B2P3R3	272	9:35	9.4		0.465684	64.06552	0.63	137.5728	22823
6B1P1R1	276	9:54	5.8	6.1	0.331755	96.20967	0.55	290.0026	5885
6B1P1R2	276	10:02	5.5	6.5	0.2241	88.24387	0.28	393.7706	708
6B1P1R3	276	10:10	5.6	6.1	0.317591	97.95325	0.46	308.4259	1426
6B1P2R1	276	10:18	5.5	6.1	0.251992	98.23186	0.53	389.8218	5104
6B1P2R2	276	10:25	5.5	6.1	0.276251	91.29197	0.49	330.4673	3310
6B1P2R3	276	10:33	5.5	6.3	0.292482	103.3761	0.38	353.4441	1855
6B1P3R1	276	10:41	5.5	6.2	0.317764	34.56523	0.62	108.7764	48246
6B1P3R2	276		5.5	6.1	0.315074	39.4246	0.56	125.1283	20937

6B1P3R3	276	10:55	5.4	6.2	0.313568	43.4756	0.55	138.6481	11411
6B2P1R1	276	11:08	5.7	6.5	0.329501	39.34321	0.64	119.4023	34917
6B2P1R2	276	11:16	5.5	6.5	0.338591	36.24048	0.61	107.0331	36152
6B2P1R3	276	11:30	5.9	6.6	0.264731	62.14801	0.6	234.7592	11899
6B2P2R1	276	11:37	6	6.7	0.289106	67.8805	0.48	234.7947	10728
6B2P2R2	276	11:46	6.1	6.7	0.332536	41.12594	0.59	123.6737	30040
6B2P2R3	276	11:53	6.1	7.1	0.323608	33.1735	0.63	102.5114	14045
6B2P3R1	276	12:01	6.1	7.3	0.278149	67.98614	0.54	244.4231	9883
6B2P3R2	276	12:09	6.5	7.2	0.29569	78.60889	0.5	265.8492	8485
6B2P3R3	276	12:17	6.4	7.3	0.28059	103.317	0.46	368.2136	5332
7B1P1R1	286	6:21	1.60	3.3	0.290221	16.6038	0.68	57.21087	14630
7B1P1R2	286	6:28	1.80	3.4	0.279827	52.75996	0.65	188.5451	5429
7B1P1R3	286	6:36	2.30	3.7	0.280673	23.15372	0.66	82.49363	11476
7B1P2R1	286	6:45	2.30	3.6	0.303602	41.94984	0.67	138.174	5429
7B1P2R2	286	6:53	2.10	3.4	0.26627	21.31783	0.68	80.06108	16873
7B1P2R3	286	7:02	2.30	3.1	0.315732	35.90335	0.65	113.7146	6730
7B1P3R1	286	7:11	2.40	3.4	0.261304	51.93341	0.67	198.747	5201
7B1P3R2	286	7:19	2.10	3.4	0.299681	47.49432	0.58	158.4832	4291
7B1P3R3	286	7:26	2.20	3.4	0.24321	51.17685	0.55	210.4222	4096
7B2P1R1	286	7:49	2.40	3.7	0.308529	68.34573	0.6	221.521	5169
7B2P1R2	286	7:56	2.20	3.5	0.33064	74.89698	0.61	226.5212	4454
7B2P1R3	286	8:04	2.40	3.5	0.363629	58.84803	0.66	161.8352	8908
7B2P2R1	286	8:13	2.40	3.6	0.284522	84.87835	0.53	298.3187	3041
7B2P2R2	286	8:21	2.70	3.5	0.318706	85.09763	0.55	267.0095	3370
7B2P2R3	286	8:30	2.50	3.6	0.218246	80.51273	0.49	368.9085	2363
7B2P3R1	286	8:38	2.50	3.6	0.379598	70.85328	0.63	186.6533	6112
7B2P3R2	286	8:46	2.50	3.7	0.26062	92.68329	0.44	355.6268	2782
7B2P3R3	286	8:53	2.60	3.8	0.318267	84.01729	0.57	263.9834	4487
8B1P1R1	289	8:08	4.9	4.9	0.371421	90.44559	0.65	243.5121	1864
8B1P1R2	289	8:16	4.9	4.8	0.331869	34.02605	0.69	102.5286	12647
8B1P1R3	289	8:24	4.8	4.8	0.345991	112.2928	0.6	324.5545	2064
8B1P2R1	289	8:34	4.7	4.8	0.329442	47.00207	0.66	142.6716	10501
8B1P2R2	289	8:41	4.8	4.9	0.349152	105.3058	0.6	301.6043	2343

8B1P2R3	289	8:49	5.1	4.9	0.213428	126.2174	0.65	591.3824	5852
8B1P3R1	289	8:58	4.8	4.9	0.395877	60.08369	0.65	151.7738	8648
8B1P3R2	289	9:05	4.9	5	0.386548	51.60023	0.66	133.4898	11282
8B1P3R3	289	9:12	4.8	4.9	0.353252	39.1487	0.66	110.8239	8322
8B2P1R1	289	9:31	5.2	5.1	0.40123	70.6928	0.65	176.1902	10631
8B2P1R2	289	9:39	5	5.2	0.339417	112.7412	0.55	332.1615	2452
8B2P1R3	289	9:47	5.4	5.1	0.299985	139.2245	0.6	464.1048	3738
8B2P2R1	289	9:55	4.9	5.2	0.323728	132.2498	0.59	408.5212	2313
8B2P2R2	289	10:02	5.5	5.2	0.408027	62.64131	0.65	153.5224	12159
8B2P2R3	289	10:10	5.5	5.2	0.331338	118.5564	0.59	357.8109	2003
8B2P3R1	289	10:19	5.2	5.3	0.354726	85.43851	0.57	240.8578	7315
8B2P3R2	289	10:26	5.6	5.3	0.388685	80.63269	0.61	207.4497	8551
8B2P3R3	289	10:34	5.7	5.3	0.350389	117.8074	0.59	336.2192	6112
9B1P1R1	300	6:11	3	3.2	0.149806	20.02116	0	133.647	63916
9B1P1R2	300	6:24	2.9	3.2	0.307387	34.19833	0.67	111.2549	5299
9B1P1R3	300	6:31	2.7	3	0.301802	47.11781	0.65	156.1218	3348
9B1P2R1	300	6:41	2.8	3	0.309923	58.29665	0.62	188.1006	2154
9B1P2R2	300	6:49	2.8	3	0.319775	59.07888	0.64	184.7516	2393
9B1P2R3	300	6:57	3	3.1	0.286675	60.72114	0.62	211.8116	2493
9B1P3R1	300	7:06	3	3	0.211565	8.083601	0.62	38.20868	19961
9B1P3R2	300	7:15	2.9	2.9	0.263861	19.67584	0.7	74.56905	19117
9B1P3R3	300	7:25	2.7	2.9	0.269798	73.45812	0.59	272.2712	1645
9B2P1R1	300	7:38	2.9	3	0.272596	90.61526	0.61	332.4155	1386
9B2P1R2	300	7:45	2.6	3	0.305449	73.28751	0.65	239.9339	2672
9B2P1R3	300	7:54	2.6	3	0.28131	84.91803	0.61	301.8661	1755
9B2P2R1	300	8:02	2.6	3	0.359141	64.40784	0.71	179.3388	5104
9B2P2R2	300	8:09	2.8	3	0.266636	74.82583	0.53	280.6292	1117
9B2P2R3	300	8:17	2.8	3	0.285388	89.343	0.61	313.0578	1516
9B2P3R1	300	8:26	2.8	2.8	0.309269	100.4443	0.58	324.7799	1755
9B2P3R2	300	8:34	3	3	0.380779	90.28745	0.63	237.1126	2762
9B2P3R3	300	8:42	2.8		0.253894	99.12274	0.45	390.4104	1059
10B1P1R1	305	7:54	1.5	2.4	0.316685	30.40575	0.67	96.01271	9655
10B1P1R2	305	8:01	1.5	2.4	0.366853	49.75624	0.65	135.6299	3230

10B1P1R3	305	8:09	1.4	2.4	0.367809	40.89278	0.65	111.1794	4259
10B1P2R1	305	8:18	1.5	2.4	0.381067	41.25784	0.65	108.2691	6924
10B1P2R2	305	8:25	2.3	2.4	0.379175	49.62767	0.66	130.8835	5689
10B1P2R3	305	8:33	1.8	2.4	0.309051	106.9012	0.49	345.9016	1386
10B1P3R1	305	8:42	1.5	2.2	0.328993	14.10803	0.69	42.88252	37550
10B1P3R2	305	8:49	1.5	2.3	0.363959	38.1587	0.68	104.8434	13720
10B1P3R3	305	8:57	1.6	2.3	0.32997	73.86109	0.59	223.842	4779
10B2P1R1	305	9:26	1.7	2.3	0.377332	100.5081	0.62	266.3655	4063
10B2P1R2	305	9:34	1.8	2.3	0.386525	26.73451	0.68	69.16633	27927
10B2P1R3	305	9:41	1.8	2.3	0.368743	101.9312	0.6	276.4291	3771
10B2P2R1	305	9:49	1.8	2.3	0.371598	40.05768	0.65	107.7983	5137
10B2P2R2	305	9:57	1.7	2.3	0.286355	130.9322	0.47	457.2369	1894
10B2P2R3	305	10:04	1.8	2.3	0.362088	43.01825	0.66	118.806	18986
10B2P3R1	305	10:12	1.6	2.5	0.374156	101.5352	0.62	271.3712	4747
10B2P3R2	305	10:20	1.8	2.4	0.362225	44.43089	0.65	122.6612	16971
10B2P3R3	305	10:27	1.7	2.3	0.332223	113.6597	0.58	342.1192	3210
11B1P1R1	310	12:45	2.9	2.5	0.38265	59.2728	0.63	154.9007	5169
11B1P1R2	310	12:52	3	2.4	0.363604	39.53821	0.64	108.7398	9005
11B1P1R3	310	12:59	2.7	2.3	0.377545	40.84427	0.64	108.1838	9396
11B1P2R1	310	13:08	2.9	2.4	0.362795	18.37492	0.64	50.64825	31536
11B1P2R2	310	13:15	2.9	2.3	0.296486	48.6035	0.56	163.9317	7412
11B1P2R3	310	13:22	2.8	2.4	0.342053	26.92885	0.6	78.72707	15735
11B1P3R1	310	13:31	2.7	2.4	0.343631	18.25876	0.63	53.13484	15410
11B1P3R2	310	13:38	2.4	2.3	0.359364	43.05389	0.64	119.8057	7477
11B1P3R3	310	13:46	2.4	2.4	0.336548	29.40192	0.67	87.36326	12419
11B2P3R1	310	13:56	2.3	3.2	0.360304	64.38946	0.63	178.7088	3544
11B2P3R2	310	14:03	2.9	3.1	0.368777	96.38751	0.61	261.3709	3446
11B2P3R3	310	14:11	2.9	3.2	0.373645	64.07733	0.66	171.4924	5754
12B1P1R1	314	16:31	1	0.9	0.347494	64.32983	0.68	185.1252	1964
12B1P1R2	314	16:38	0.7	1	0.295716	23.35223	0.71	78.96841	9915
12B1P1R3	314	16:45	1.1	1.1	0.329244	47.03811	0.68	142.8672	3901
12B1P2R1	314	16:54	1.2	1.1	0.338232	68.93961	0.64	203.8237	1875
12B1P2R2	314	17:01	1.2	1.1	0.324674	70.16497	0.59	216.1087	1015

12B1P2R3	314	17:09	1.1	1.1	0.311237	31.41706	0.7	100.9427	7152
12B1P3R1	314	17:18	1.2	1.1	0.234269	11.83569	0.7	50.52175	15638
12B1P3R2	314	17:26	1.3	1.1	0.289503	36.89821	0.64	127.4538	4747
12B1P3R3	314	17:34	1.2	1.1	0.238486	10.21335	0	42.82582	52960
12B2P1R1	314	17:52	1.4	1.8	0.327791	73.60402	0.69	224.5456	2842
12B2P1R2	314	18:00	1.2	1.8	0.282619	30.1937	0.73	106.8354	9786
12B2P1R3	314	18:07	1.4	1.8	0.277096	16.7976	0.71	60.62022	17751
12B2P2R1	314	18:15	1.2	1.8	0.339825	39.25342	0.7	115.5106	4649
12B2P2R2	314	18:22	1.1	1.8	0.33121	47.01285	0.69	141.9428	5137
12B2P2R3	314	18:30	1.1	1.7	0.327139	67.94256	0.66	207.6874	2782
12B2P3R1	314	18:38	0.9	1.6	0.329743	57.78805	0.68	175.2521	3219
12B2P3R2	314	18:45	0.7	1.7	0.329672	48.42366	0.69	146.8844	2543
12B2P3R3	314	18:53	1.2	1.5	0.322479	46.75776	0.71	144.9948	5266
13B1P1R1	319	7:11	-0.5	-1	0.30375	41.8155	0.62	137.6644	1984
13B1P1R2	319	7:18	-0.9	-0.4	0.343144	48.62541	0.75	141.7054	4486
13B1P1R3	319	7:28	-1.1	-0.7	0.322906	49.53654	0.67	153.4084	1496
13B1P2R1	319	7:35	-1.1	-0.4	0.31463	63.90024	0.61	203.0962	878
13B1P2R2	319	7:43	-1.1	-0.7	0.200333	9.375294	0.7	46.79864	19897
13B1P2R3	319	7:51	-0.9	-0.4	0.263207	65.37094	0.64	248.3633	1037
13B1P3R1	319	8:00	-0.5	-0.4	0.275502	14.65741	0.75	53.2025	18109
13B1P3R2	319	8:08	-0.6	-0.8	0.324311	43.34422	0.72	133.6502	2403
13B1P3R3	319	8:16	-0.8	-0.6	0.179386	6.229696	0.72	34.72782	12257
13B2P1R1	319	8:29	-0.8	-0.4	0.347624	58.76646	0.7	169.0517	2592
13B2P1R2	319	8:37	-0.3	0.3	0.359249	58.92201	0.69	164.0146	2891
13B2P1R3	319	8:44	-0.6	0	0.334485	84.47618	0.74	252.556	3316
13B2P2R1	319	8:52	-0.6	0.1	0.354609	36.40447	0.7	102.6608	5202
13B2P2R2	319	8:59	-0.9	-0.1	0.358316	41.65613	0.72	116.2554	6600
13B2P2R3	319	9:06	-0.8	0	0.404113	29.01081	0.74	71.78883	12582
13B2P3R1	319	9:14	-0.3	0.1	0.349578	101.6385	0.6	290.7465	1466
13B2P3R2	319	9:22	-0.3	0.1	0.374196	56.60596	0.68	151.2734	3641
13B2P3R3	319	9:30	-0.4	0.1	0.329713	102.0044	0.53	309.3735	1236
14B1P1R1	325	12:24	-2	-1.9	0.381063	70.13562	0.61	184.0526	1725
14B1P1R2	325	12:32	-1.8	-2	0.393577	51.29259	0.64	130.324	3284

14B1P1R3	325	12:40	-2	-1.9	0.377182	36.07392	0.68	95.64057	2702
14B1P2R1	325	12:48	-2	-1.9	0.396801	55.29224	0.65	139.3452	3348
14B1P2R2	325	12:56	-2	-2	0.318432	24.09776	0.66	75.67639	17849
14B1P2R3	325	13:03	-1.5	-2	0.35894	77.94983	0.62	217.1667	1884
14B1P3R1	325	13:12	-1.5	-2.2	0.389885	33.58338	0.66	86.1367	11996
14B1P3R2	325	13:20	-1.5	-2	0.376095	59.04028	0.65	156.9825	2652
14B1P3R3	325	13:27	-1.4	-2	0.43687	48.9312	0.67	112.004	5234
14B2P1R1	325	13:43	-0.9	-0.7	0.370332	42.97358	0.7	116.0408	7380
14B2P1R2	325	13:51	-1.2	-0.1	0.381471	34.34002	0.7	90.02013	16060
14B2P1R3	325	13:59	-1.3	-0.1	0.369545	89.45816	0.7	242.0766	1436
14B2P2R1	325	14:07	-1.2	-1.2	0.421326	35.47071	0.71	84.18828	4519
14B2P2R2	325	14:15	-1.4	-0.2	0.357742	74.49651	0.71	208.2409	2353
14B2P2R3	325	14:22	-1.3	-0.2	0.403113	66.97796	0.7	166.1517	2812
14B2P3R1	325	14:31	-1.2	-0.2	0.372663	42.95548	0.69	115.2663	4292
14B2P3R2	325	14:41	-2	-1.1	0.436347	48.03251	0.69	110.0788	5397
14B2P3R3	325	14:49	-2	-0.1	0.367533	78.66403	0.69	214.0326	2114
15B1P1R1	334	7:44	-2.2	-1.9	0.266544	15.54445	0.7	58.31852	3608
15B1P1R2	334	7:53	-2.5	-2	0.232984	12.13937	0.72	52.10392	5264
15B1P1R3	334	8:01	-3.2	-2.1	0.230925	9.978595	0.7	43.21143	3111
15B1P2R1	334	8:13	-3.3	-2	0.250879	13.35986	0.7	53.25229	4519
15B1P2R2	334	8:21	-3.3	-2	0.253657	13.74512	0.71	54.18784	4259
15B1P2R3	334	8:29	-3.7	-2	0.282505	46.0457	0.67	162.9909	1092
15B1P3R1	334	8:37	-3.2	-2.1	0.295591	13.3397	0.77	45.12896	24805
15B1P3R2	334	8:44	-3.5	-2	0.209951	7.596902	0.72	36.18418	5787
15B1P3R3	334	8:51	-3.7	-2.1	0.270093	45.97105	0.64	170.2043	769
15B2P1R1	334	9:17	-3.6	-1.9	0.333442	40.65077	0.68	121.9127	1226
15B2P1R2	334	9:24	-3.2	-1.3	0.337191	27.12248	0.73	80.43651	2612
15B2P1R3	334	9:33	-3.3	-1.7	0.355742	34.85078	0.71	97.96655	1845
15B2P2R1	334	9:41	-3	-1.4	0.279072	17.75863	0.73	63.6347	8388
15B2P2R2	334	9:50	-3	-1.3	0.328222	26.69944	0.73	81.34569	5559
15B2P2R3	334	9:58	-3.1	-1.4	0.354915	19.59638	0.72	55.21435	5656
15B2P3R1	334	10:08	-3.6	-0.1	0.380533	44.28616	0.7	116.3792	2104
15B2P3R2	334	10:15	-3.4	-0.1	0.302522	54.2712	0.68	179.3959	1755

15B2P3R3	334	10:26	-3.2	-0.1	0.346735	23.11703	0.72	66.67063	6112
16B1P1R1	341	14:03	-2.8	-2.5	0.193725	72.37438	0.69	373.5943	8843
16B1P1R2	341	14:10	-2.7	-2.4	0.26639	24.04675	0.47	90.26899	7510
16B1P1R3	341	14:18	-3	-2.5	0.224336	67.96865	0.37	302.977	6047
16B1P2R1	341	14:26	-2.8	-1.9	0.199383	72.46418	0.67	363.4428	1436
16B1P2R2	341	14:34	-2.8	-2.6	0.201352	45.23449	0.64	224.6538	852
16B1P2R3	341	14:41	-3	-2.6	0.282283	44.53164	0.65	157.7555	874
16B1P3R1	341	14:50	-3.1	-2.2	0.235665	23.50566	0.64	99.74201	769
16B1P3R2	341	14:58	-3.1	-2.6	0.226344	17.13021	0.63	75.68213	680
16B1P3R3	341	15:06	-3.2	-2.1	0.289668	71.98857	0.71	248.5212	3804
16B2P1R1	341	15:18	-2.6	-2	0.32817	25.82978	0.71	78.70847	1795
16B2P1R2	341	15:26	-2.9	-2	0.165314	93.13573	0.67	563.3875	821
16B2P1R3	341	15:33	-2.9	-2	0.320271	30.35705	0.58	94.7854	546
16B2P2R1	341	15:41	-2.7	-2.4	0.310231	47.5641	0.71	153.3181	6372
16B2P2R2	341	15:49	-2.6	-2	0.19091	20.76022	0.63	108.7436	763
16B2P2R3	341	15:57	-2.8	-2.4	0.223666	73.4027	0.66	328.1804	1027
16B2P3R1	341	16:05	-2.7	-2.4	0.190813	4.505399	0.68	23.61156	957
16B2P3R2	341	16:13	-2.9	-2.4	0.246884	994.6192	0.66	4028.686	891
16B2P3R3	341	16:20	-2.9	-2.4	0.192501	3.421527	0.6	17.77406	549
17B1P1R1	348	6:55	-3.6	-2.6	0.17908	7.016386	0.69	39.18013	8843
17B1P1R2	348	7:02	-3.6	-2.6	0.222877	8.449975	0.47	37.91321	7510
17B1P1R3	348	7:10	-3.7	-2.6	0.217956	8.580257	0.37	39.36701	6047
17B1P2R1	348	7:18	-3.8	-2.6	0.246642	11.99543	0.67	48.63505	1436
17B1P2R2	348	7:25	-3.7	-2.6	0.245609	27.05783	0.64	110.1662	852
17B1P2R3	348	7:33	-3.7	-2.5	0.272898	18.21973	0.65	66.76385	874
17B1P3R1	348	7:41	-3.7	-2.6	0.230149	36.85711	0.64	160.1449	769
17B1P3R2	348	7:49	-3.7	-2.6	0.278622	26.20964	0.63	94.06868	680
17B1P3R3	348	7:56	-3.7	-2.6	0.291832	11.59388	0.71	39.72795	3804
17B2P1R1	348	8:07	-3.4	-1.9	0.30612	21.31862	0.71	69.64139	1795
17B2P1R2	348	8:15	-3.7	-2	0.263948	42.6044	0.67	161.4123	821
17B2P1R3	348	8:23	-3.6	-1.7	0.268008	56.20623	0.58	209.7182	546
17B2P2R1	348	8:31	-3.6	-2.1	0.192369	12.52821	0.71	65.1259	6372
17B2P2R2	348	8:41	-3.6	-2.1	0.258916	50.94481	0.63	196.7621	763
17B2P2R3	348	8:49	-3.5	-2.1	0.288102	22.66686	0.66	78.67661	1027
17B2P3R1	348	8:58	-3.6	-0.3	0.300878	31.92498	0.68	106.1061	957
17B2P3R2	348	9:06	-3.6	-0.3	0.287458	29.95981	0.66	104.2231	891
17B2P3R3	348	9:13	-3.6	-0.4	0.255314	57.4906	0.6	225.1762	549